Journal of *Marine Science and Engineering*

MDPI

Article

The Sedimentary Record of Marine–Continental Transitional Shales in the Upper Triassic of Xujiahe Formation, Southeast Sichuan Basin, China

Hao Huang [1,2], Tingshan Zhang [1,2,*], Xi Zhang [1,2,*], Yulong Liu [1,2], Lubiao Gao [1,2] and Jingxuan Zhang [3]

[1] State Key Laboratory of Oil and Gas Reservoir Geology and Exploitation, Southwest Petroleum University, Chengdu 610500, China; susehuanghao@163.com (H.H.); 15298230411@163.com (Y.L.); 15293725286@163.com (L.G.)
[2] School of Geoscience and Technology, Southwest Petroleum University, Chengdu 610500, China
[3] School of Engineering, Royal Melbourne Institute of Technology University, GPO Box 2476, Melbourne, VIC 3001, Australia; jingxuan.zhang@rmit.edu.au
* Correspondence: zts_3@126.com (T.Z.); zhangx@swpu.edu.cn (X.Z.)

Abstract: Marine–continental transitional shale is a focus of global energy exploration, offering significant but underexplored hydrocarbon potential. Unlike well-studied marine shales, these deposits pose challenges due to complex interactions between marine and continental influences. The lower Xujiahe Formation in the southeastern Sichuan Basin exemplifies this uncertainty, with its depositional environment debated as either continental or transitional. Resolving this issue is critical for refining facies models and improving exploration strategies. This study aims to determine the depositional environment of the lower Xujiahe Formation by integrating sedimentological, paleontological, and geochemical evidence. Field observations identify tidal rhythmites, reverse cross-stratification, and double mud drapes, indicative of tidal influence. Fossil assemblages, including *Sulcusicystis* sp. and marine-influenced sporopollen sequences, further support marine influence and align with records from the Tanba and Qilixia sections in northeastern Sichuan. Geochemical analysis reveals Sr concentrations (24.47–194.43 ppm), Sr/Ba ratios (0.11–0.65), m-values (4.37–33.08), and CaO/(Fe + CaO) ratios (0.03–0.80), suggesting freshwater to brackish conditions. V/Cr (0.92–2.22) and U/Th (0.18–0.48) ratios indicate a weakly oxidizing environment. Kerogen analysis classifies the organic matter as type II_2–III, suggesting periodic marine influence during deposition. These findings confirm that the lower Xujiahe Formation represents a marine–continental transitional facies, refining previous facies interpretations and providing a basis for more targeted shale gas exploration in the Sichuan Basin and comparable basins worldwide.

Keywords: marine–continental transitional environment; sedimentary structure; sporopollen; fossil; paleosalinity; paleo-oxidation–reduction

check for updates

Academic Editor: Antoni Calafat

Received: 17 February 2025
Revised: 11 March 2025
Accepted: 22 March 2025
Published: 24 March 2025

Citation: Huang, H.; Zhang, T.; Zhang, X.; Liu, Y.; Gao, L.; Zhang, J. The Sedimentary Record of Marine–Continental Transitional Shales in the Upper Triassic of Xujiahe Formation, Southeast Sichuan Basin, China. *J. Mar. Sci. Eng.* **2025**, *13*, 646. https://doi.org/10.3390/jmse13040646

Copyright: © 2025 by the authors. Licensee MDPI, Basel, Switzerland. This article is an open access article distributed under the terms and conditions of the Creative Commons Attribution (CC BY) license (https://creativecommons.org/licenses/by/4.0/).

1. Introduction

The success of shale gas development in North America has sparked a global surge in shale gas exploration. Initially, research and exploration efforts were primarily focused on marine shale, while relatively little attention was given to transitional facies. However, transitional facies shale is widely distributed and holds significant energy potential. Scholars recognize that these deposits will become a critical frontier for future shale gas exploration and development, serving as an important successor to conventional shale gas resources [1]. In recent years, continuous advancements in exploration technologies have

led to significant progress in the development of transitional facies shale gas worldwide. As a pioneer in this field, North America has achieved major breakthroughs in transitional facies shale gas production. For instance, commercially viable transitional facies shale gas has been developed in parts of the Marcellus and Utica Shales within the Appalachian Basin. Similarly, Argentina's Vaca Muerta Shale and Australia's Cooper Basin also contain transitional facies shale gas resources, with exploration and pilot development efforts steadily advancing.

In China, exploratory efforts for transitional facies shale gas have been conducted in the Sichuan and Ordos Basins. Notably, the Longtan Formation in the Sichuan Basin and the Shanxi Formation in the Ordos Basin have both demonstrated promising resource potential [2–4]. Within the Sichuan Basin, three sets of black mud-shale deposits occur in the first, third, and fifth members of the Xujiahe Formation. These deposits have garnered increasing attention due to their substantial thickness and high total organic carbon (TOC) content [5,6]. Historically, they have been studied as key continental source rocks [7]. However, drilling results in the Sichuan Basin consistently indicate that shale intervals within the Xujiahe Formation exhibit significant gas potential, highlighting the prospectivity of these deposits for shale gas exploration.

The gaps in the current study are as follows: (1) Despite the widespread distribution of the Xujiahe Formation across the Sichuan Basin and its adjacent regions, its sedimentary facies remain a subject of ongoing debate. Previous studies have primarily classified the formation as a continental clastic deposit [8–12]. (2) However, field outcrops reveal the presence of both terrestrial plant fossils and marine or marine-influenced taxa, such as brachiopods and small spiny algae. This raises key questions about the depositional environment of the formation and the extent of marine influence. (3) Additionally, a lack of integrated sedimentological, paleontological, and geochemical analyses has hindered a comprehensive understanding of its depositional conditions. Addressing these gaps is crucial for improving stratigraphic correlations and resource assessments.

The significance of the study is as follows: (1) Clarifying the depositional environment of the Xujiahe Formation has significant implications for both geological research and resource exploration. Understanding whether these shales represent marine–continental transitional facies will refine depositional models and provide new insights into sedimentary processes in similar settings worldwide. (2) Moreover, an improved understanding of the formation's facies distribution can enhance shale-gas-prospecting strategies, guiding future exploration efforts in the Sichuan Basin and beyond. (3) This study also contributes to the broader understanding of transitional facies and their potential as viable shale gas reservoirs, supporting more targeted and efficient resource extraction in comparable geological settings.

This study focuses on multiple outcrop sections in the southeastern Sichuan Basin to investigate the depositional environment of the organic-rich mud shale within the Xujiahe Formation. By integrating field observations, paleontological evidence, and geochemical analyses, this research aims to clarify the sedimentary characteristics of these deposits and provide new insights for hydrocarbon exploration in similar transitional facies worldwide.

2. Geologic Setting

Located at the western periphery of the Yangtze Plate and the eastern margin of the ancient Tethys Ocean [13,14], Sichuan Basin is identified as a foreland basin formed by the overthrust of the Songpan–Ganzi tectonic belt to the western periphery of the Yangtze Plate amid the Late Triassic Paleo-Tethys Ocean's closure [15,16] (Figure 1). From the Ediacaran to the Late Triassic Carnian, the western periphery of the Yangtze Plate functioned as a marine carbonate platform on a passive continental margin [17,18]. During the Late Triassic period,

it transitioned to the Xujiahe Fm, characterized by terrigenous clastic deposits in a foreland basin [19]. The Xujiahe Fm played an important role of stratum that records the tectonic transformation of the western periphery of the Yangtze Plate and the early formation of the Longmenshan foreland basin [20]. It effectively recorded the paleoenvironmental changes during the gradual transformation of the Sichuan basin from a passive continental margin to a foreland basin [21].

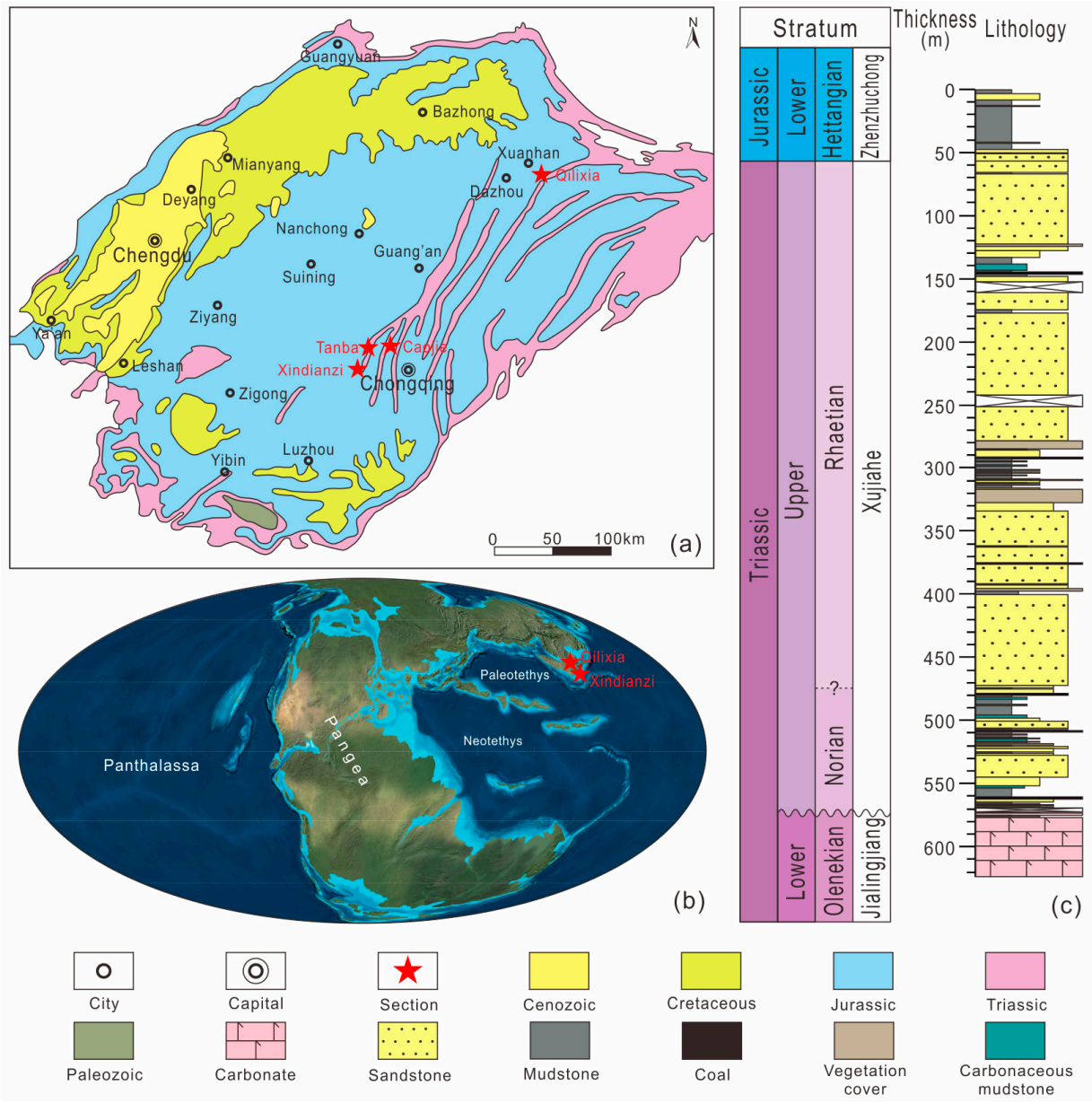


Figure 1. Paleogeographic pattern of the Late Triassic period and location of research section. (**a**) Essential geological map of the Sichuan Basin; (**b**) Late Triassic paleogeographic pattern [22]; (**c**) stratigraphic scheme and lithology of Xujiahe Fm in Sichuan Basin (modified from Lu et al., 2023) [23].

During the Late Triassic, the overall paleogeographic characteristics of the Sichuan Basin were dominated by a large plain or peneplain, with higher elevations in the southeast and lower elevations in the northwest. During this period, the northwestern part of the basin was adjacent to the sea [24]. The sedimentation in this stage is mainly continental, but with the rise and fall of the sea level or the crust, the sea water can quickly spread to most areas of the plain. From the west part to the southeastern of Sichuan basin, the system of the lacustrine basin gradually transitioned to the near-source delta system [25]. The

Luzhou palaeouplift, located in the southeast of the basin, sprouted in the Early Triassic and disappeared in the Late Triassic, acted as a barrier during the transgression period [26].

The southeastern Sichuan Basin is positioned at the junction of two second-order tectonic units [27], the fold structures with low steepness in South Sichuan and high steepness in East Sichuan, and the fold structure is very developed under the influence of the Huaying Mountain broom-like tectonic system [28]. The Xujiahe Fm in the southeast part of Sichuan Basin is a set of slowly subsiding strata that were formed under the combined control of the Longmen Mountain Fault Zone during the Middle to Late Indosinian period, crustal loading on the southern Qinling Mountain, and continental compression orogeny in the Xuefeng Mountain [12,29–32]. This formation overlies the Middle Triassic carbonate rocks.

The thickness of Upper Triassic Xujiahe Fm in the Sichuan Basin increases progressively from the southeast to the northwest, and the sedimentary thickness reaches 500–600 m in the Yongchuan area, which reflects that the eastern part of the study area is elevated, while the western part is relatively lower. The Xujiahe Fm in the study area is thin only in the high part of Luzhou palaeouplift, and the minimum thickness is about 300 m [33]. According to the seismic profile, the southeastern Sichuan Basin received sediments in the early Xujiahe Fm, but due to the influence of the Luzhou palaeouplift, the sediments in the high parts of the palaeouplift were thin or partially subjected to denudation (Figure 2). Generally, the strata of Xujiahe Fm from the first to sixth members in the southeastern Sichuan Basin are relatively intact.

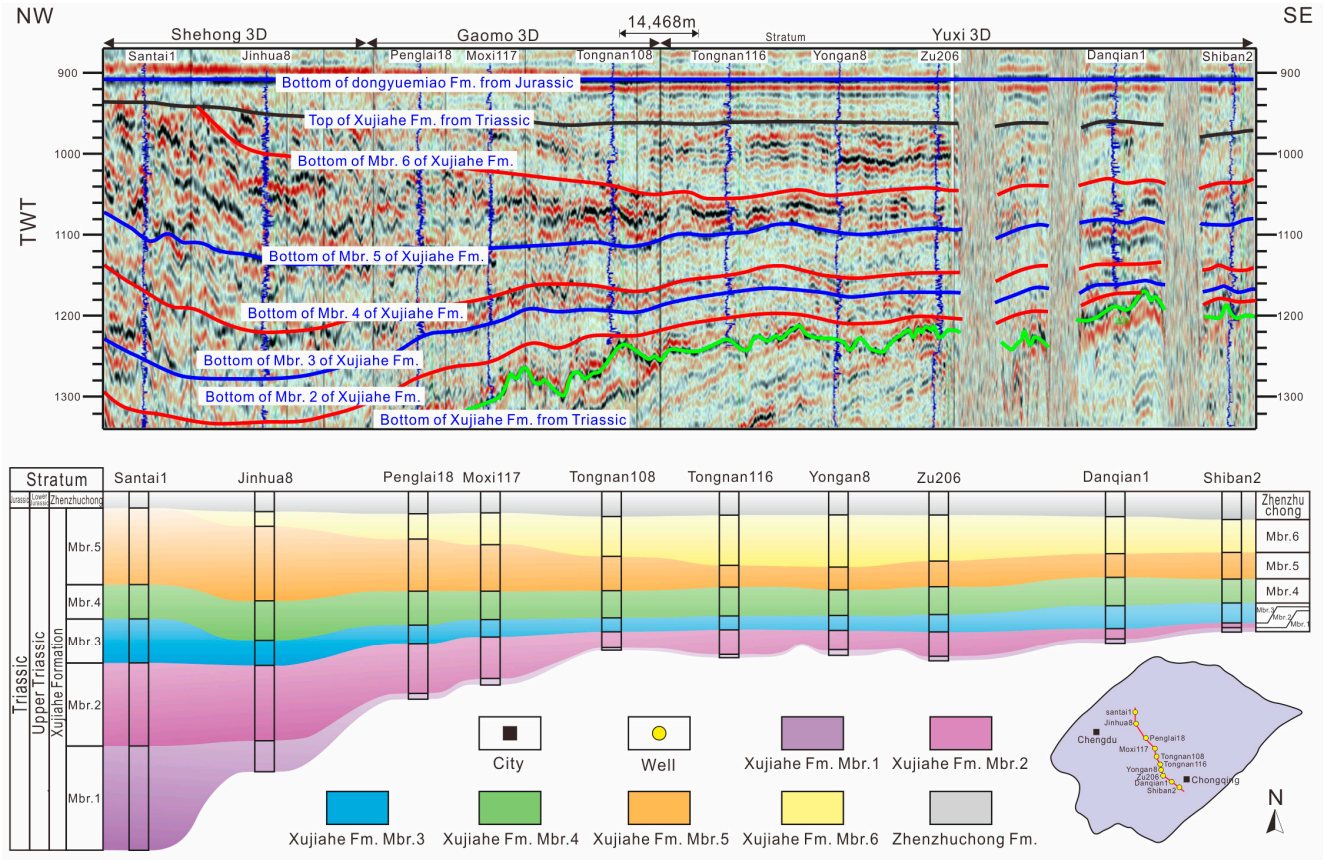


Figure 2. Stratigraphic correlation map of Upper Triassic Xujiahe Fm in Sichuan Basin.

Throughout the Xujiahe Fm's sedimentary period, the basin underwent significant fluctuations in water level, and the sand and mud layers appeared alternately due to the alternating sea (lake) transgression and sea (lake) regression [9,34]. The lithology of the whole stratum is mainly composed of gray to dark-gray mud shale and light-gray

fine sandstone. The underlying stratum of Xujiahe Fm is the dolomite of Middle Triassic Jialingjiang Formation, and the contact relation is unconformity contact. The overlying stratum is a set of quartz sandstone transition layer and the purple mudstone of Lower Jurassic Ziliujing Formation, and the contact relation is parallel unconformity [35]. The Xujiahe Fm can be subdivided into six lithological segments. Specifically, the second, fourth, and sixth units are primarily composed of light-gray siltstone and gray-to-white fine sandstone, whereas the first, third, and fifth units consist predominantly of gray–black shale interbedded with dark gray mudstone and siltstone.

The organic-rich shale in Member (Mbr) 1 of the Xujiahe Formation (Fm), located in the southeastern Sichuan Basin, is the main research target for understanding the marine–continental transitional facies of the Early Xujiahe Fm. Based on the findings from section analysis, Mbr 1 of the Xujiahe Fm can be further subdivided into two distinct submembers, which are SubMember (SubMbr) 1 of Mbr 1 from the Xujiahe Fm and SubMbr 2 of Mbr 1 from the Xujiahe Fm from the bottom up. SubMbr 1 of Mbr 1 from the Xujiahe Fm primarily consists of light gray fine-grained sandstone, siltstone, muddy siltstone and dark-gray mudstone, while SubMbr 2 of Mbr 1 from the Xujiahe Fm mainly consists of dark-gray mudstone and gray–black shale, interspersed with siltstone and fine sandstone. The marine and marine–continental transition fossils discovered in this study are located at SubMbr 2 of Mbr 1 from the Xujiahe Fm. (Figure 3).

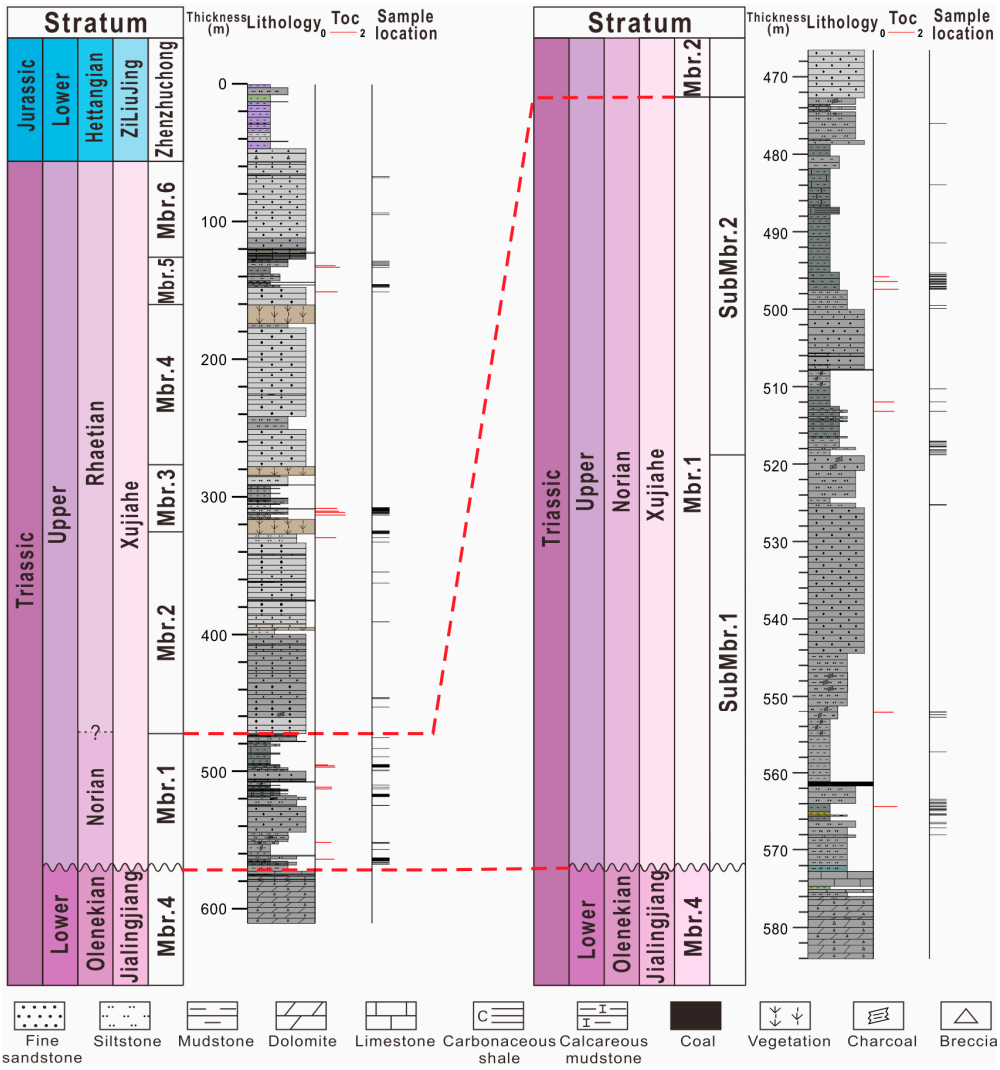


Figure 3. Stratigraphic correlation map of Xujiahe Fm in the southeast part of Sichuan Basin.

3. Materials and Methods

The samples were collected from the field outcrop of Chongqing City from Hechuan District to Yongchuan District in southeastern Sichuan Basin. The drilling core samples and cuttings samples were collected from wells in the research region. All the samples are fresh samples unaffected by weathering. Plastic bags were used to reduce samples' oxidation and avoid contamination. A total of 250 samples including shale, mudstone, and silty mudstone were collected. The particle sizes ranged from 0.01 to 0.13 mm. The methods, experimental test, and analysis we have carried out include the following: field profile observation, total organic carbon determination, kerogen maceral determination, major and trace elements determination, and sporopollen analysis. The analysis and testing were carried out in the State Key Laboratory of Oil and Gas Reservoir Geology and Exploitation, Southwest Petroleum University, China.

3.1. Field Profile Observation

In order to prove that the early stage of Xujiahe Fm in the southeastern Sichuan Basin had a marine–continental transitional facies sediment, the field profile observation centers on the "sedimentary structure of the Xujiahe Fm Mbr 1" as the primary research focus. In light of the observation and statistics of sedimentary structures with typical characteristics of transitional environment in these field section, the period and scale of marine–continental transitional sediments are defined.

3.2. Sporopollen Analysis

Sporopollen fossil samples are processed using the laboratory standard analytical method for sporopollen (SY/T 5915–2018) [36], with observations and identifications using a biological binocular microscope (model: ZEISS Scope A1, eyepiece: 10×, objective lenses: 20× and 40×). For samples rich in sporopollen fossil, at least 200 grains are counted; for relatively rich samples, 100 grains are counted or the number of 4 thin sections (20 × 20 mm); for samples with scarce fossils, the number of 8 thin sections are counted. After counting, samples with more than 60 grains are used for percentage content calculation and spectral analysis.

3.3. Major and Trace Elements Determination

The major element analysis was based on Quantification of 27 Elements, Including Calcium Oxide, Employing Inductively Coupled Plasma Atomic Emission Spectrometry (DZ/T 0279.2–2016) [37]; Methods for Chemical Analysis of Limestone and Dolomite (GB/T3286 (1–9)–2014) [38]; Part 28 of Approaches to the Chemical Analysis of Silicate Rocks: Determination of 16 Main and Trace Components (GB/T 14506.28–2010) [39], using inductively coupled plasma optical emission spectrometer (ICP–OES, PE, 5300V, Waltham, MA, USA) to complete the analysis and test.

For trace element analysis, according to the Determination of 15 Elements such as Barium, Beryllium and Bismuth (DZ/T 0279.3–2016) [40] and the Measurement of 15 Rare Earth Elements, Including Lanthanum and Cerium, Using Closed Acid Digestion–Inductively Coupled Plasma Mass Spectrometry (DZ/T 0279.32–2016) [41], the analytical test was performed with an inductively coupled plasma mass spectrometer (ICP–MS, Agilent, 7700, Santa Clara, CA, USA).

3.4. Total Organic Carbon Analysis

TOC content was analyzed according to the industry standard Determination of Total Organic Carbon in Sedimentary Rocks (GB/T 19145–2003) [42]. To remove inorganic carbon, each finely powdered sample (200 mesh) was exposed to 10% HCl at 65 °C for 20 h. The

sediment fractions were cleaned using distilled water and dried at 55 °C for over 30 h. We completed the analysis and test using carbon/sulfur analyzer (LECO, CS–230, San Jose, CA, USA).

3.5. Kerogen Maceral Determination

Industry standard "Transmission light-fluorescence kerogen maceral identification and Classification Method" (SY/T 5125-2014) [43] has been followed; transmission light microscope (Zhong Yan Jinan Test Machine Co., Ltd., K32315, Jinan, Shandong Province, China) was used for observation and identification of kerogen maceral.

4. Results

4.1. Sedimentological Characteristics

Sedimentary structures have been observed on the outcrop and core of Xujiahe Fm Mbr 1 in the Xindianzi section, Yongchuan. These sedimentary structures are helpful to restore the paleo-flow and paleo-sedimentary environment in the sedimentary basin.

In SubMbr 1 of Mbr 1 from the Xujiahe Fm, the collapse breccia at the boundary from the bottom of Xujiahe Fm to the underlying Jialingjiang Fm can be clearly seen (Figure 4e). This submember is dominated by continental sedimentary structures, such as lenticular sandbody (Figure 4c) and dual structure (Figure 4d). These sedimentary structures indicate that the sedimentary environment of the southeastern Sichuan Basin was continental in nature during the sedimentary stage of SubMbr 1 of Mbr 1 from the Xujiahe Fm.

In SubMbr 2 of Mbr 1 from the Xujiahe Fm, the continental sedimentary structure basically disappeared and was replaced by lots of marine–continental transitional sedimentary structures. In the field section, the following can be observed: positive rhythm stratification with grain size decreasing upward and bedding size decreasing upward (Figure 4f); bioturbation structures and bioboreholes (Figure 4h); vein, wavy, and lenticular bedding (Figure 4i). These sedimentary structures are consistent with the distinctive qualities of the marine–continental transitional sedimentary environment.

In order to observe more clearly some of the miniature marine–continental transitional sedimentary structures, we also drilled several core samples in SubMbr 2 of Mbr 1 from the Xujiahe Fm of the Xindianzi section and polished the samples for easy observation. On the drilled core samples, it can be clearly observed that wavy bedding (Figure 5a,e), vein bedding (Figure 5a,e), lenticular bedding (Figure 5a,d), double mud-drape structure (Figure 5a,d), swash cross-bedding (Figure 5a,d), feathery cross-bedding (Figure 5d), soft sedimentary deformation structure (Figure 5e), and other sedimentary structures indicating the marine–continental transitional sedimentary environment. A lot of sedimentary structures prove that SubMbr 2 of Mbr 1 from the Xujiahe Fm in the southeastern Sichuan Basin is a continental sedimentary, and SubMbr 2 of Mbr 1 from the Xujiahe Fm is a marine–continental transitional sedimentary.

4.2. Fossils and Sporopollen Fossil Analysis

Numerous fossils have been identified in the lower deposits of the Xujiahe Formation, exhibiting clear differentiation. The fossils found in SubMbr 1 of Mbr 1 from the Xujiahe Fm are mainly terrestrial plants such as ferns and gymnosperms, including leaf and stem fossils. In SubMbr 2 of Mbr 1 from the Xujiahe Fm, both the species and the number of terrestrial plant fossils are significantly reduced, and *Micrhystridium* sp., a marine fossil, is found in this submember. The changes of fossil species and quantity indicate that the sedimentary environment in the southeastern Sichuan Basin transformed from terrestrial environment to marine–continental transitional environment in the sedimentary epoch of Xujiahe Fm Mbr 1.

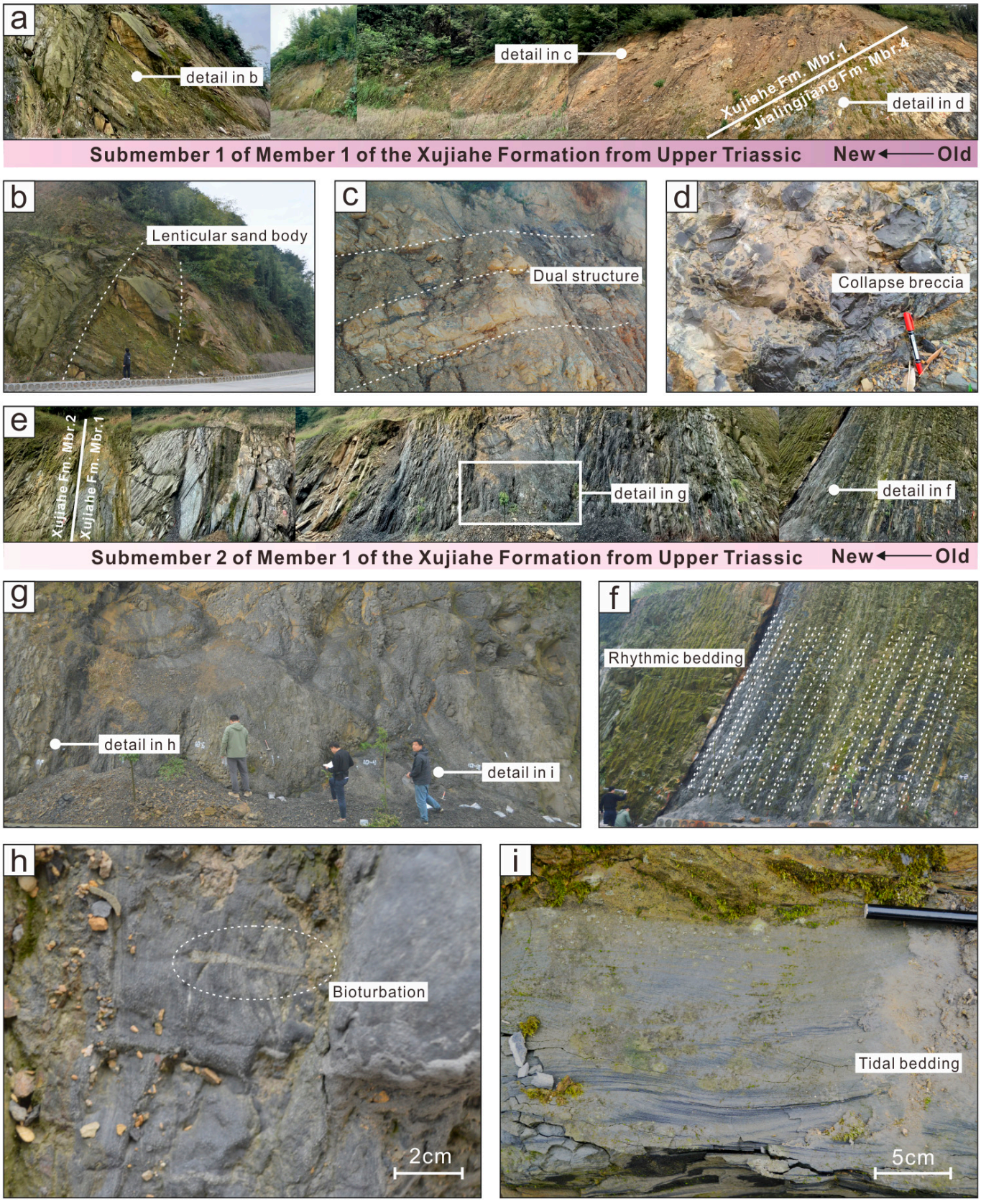


Figure 4. Typical sedimentary structure of Xujiahe Fm Mbr 1 in Xindianzi section. (**a**) SubMbr 1 of Mbr 1 from the Xujiahe Fm section panorama; (**b**) lenticular sandbody; (**c**) dual structure; (**d**) collapse breccia; (**e**) SubMbr 2 of Mbr 1 from the Xujiahe Fm section panorama; (**f**) rhythmic bedding (**g**) Close-up view of the upper part of SubMbr 2 of Mbr 1 from the Xujiahe Fm; (**h**) bioturbation; (**i**) lenticular bedding and wavy bedding.

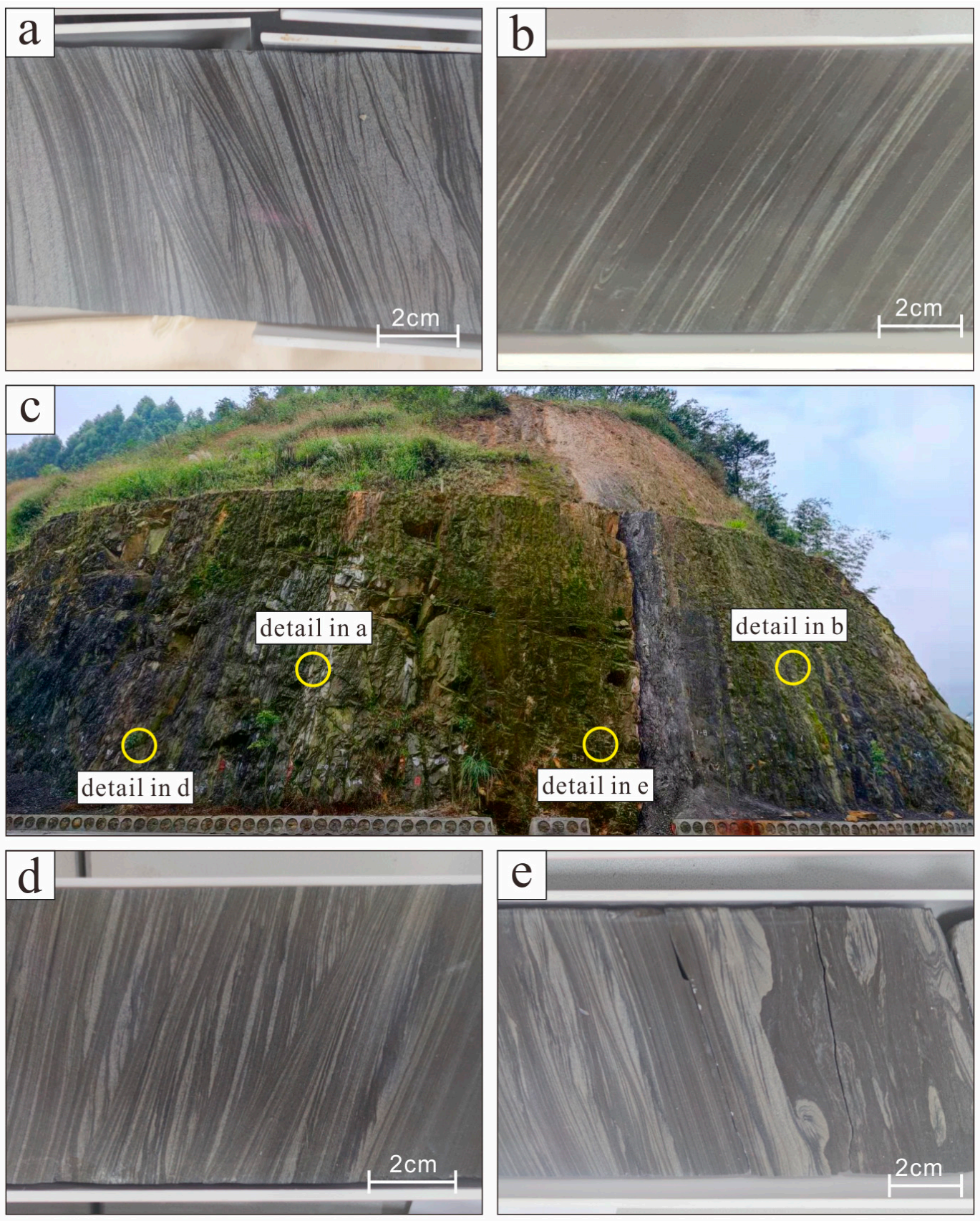


Figure 5. Typical sedimentary structure of Xujiahe Fm Mbr 1 in Xindianzi section (core sample). (**a**,**d**) Double mud-drape structure, wavy cross-bedding, lenticular bedding, and swash cross-bedding. (**b**) Rhythmic bedding. (**c**) The lower part of SubMbr 2 of Mbr 1 from the Xujiahe Fm; (**d**) Feather cross-bedding. (**e**) Soft sedimentary deformation.

The sporopollen fossils of 38 samples extracted from the lower segment of Xujiahe Fm were analyzed, including 123 species from 90 genera and undetermined species. The abundance and diversity of fossils in each sample are different, and the preservation status is also different, which can be roughly divided into two Assemblages. Assemblage I: *Dictyophyllidites harrisii–Kyrtomisporis coronarius–Chasmatosporiteshians* were distributed in SubMbr 1 of Mbr 1 from the Xujiahe Fm, moss and fern spores dominated, and gymnosperms pollen played a secondary role. The spores of moss and fern were 43.76–79.03%, with an average of 69.86%; the pollen content of gymnosperms was 16.0–56.24%, with an average of 27.78%. Assemblage II: *Aratrisporites fischeri–Taeniaesporites rhaeticus–Chasmatosporites hians*, distributed in SubMbr 2 of Mbr 1 from the Xujiahe Fm, mainly gymnosperm pollen, followed by moss and fern spores. The pollen content of gymnosperms was 44.68–78.98%, with an average of 60.76%; the spores of moss and fern were 21.02–55.32%, with an average of 39.24%.

The above two assemblages correlate with certain sporopollen assemblages from the Middle to late Late Triassic, such as those in the Xujiahe Fm of the northwestern Sichuan Basin and the Daqing Formation in the Baoding area of Sichuan Province [44], Ganhaizi Formation and Shezi Formation in Luquan–Pinglang coal measures in Yunnan Province [45], and Huobachong Formation in Liuzhilangdai in Guizhou Province [46]. In addition, this combination can also be combined with the Ritian sporopollen of the Kendelbachgraben section in Salzburg, Austria [47], the sporopollen assemblage of Höganäs Fm in NW Skane, southern Sweden [48], and the Ruteian sporopollen assemblage of Zagaji Fm in NW Poland [49] and other general comparison. The geological age of the sporopollen assemblage should be the Middle and late Late Triassic, which is roughly Norian–Rhaetian.

4.3. Element Geochemistry

4.3.1. Major Elements

A total of 30 mud-shale samples from the Xujiahe Fm were selected for analysis of major elements and trace elements. Among the major elements, the most abundant oxides were SiO_2 (48.25–82.62%, 69.22% on average) and Al_2O_3 (9.52–30.01%, 16.94% on average), followed by Fe_2O_3 (0.85 to 14.78%, on average, 4.85%), K_2O (1.55 to 6.02%, on average, 3.64%), CaO (0.06 to 22.22%, on average, 2.13%), and MgO style (0.43 to 4.40%, on average, 1.77%), and accessory oxides, including TiO_2, Na_2O, P_2O_5, and MnO, were less than 1.0%. The results of major element concentrations of the Xujiahe Fm from the Xindianzi section in Sichuan Basin are shown in Table 1.

Table 1. Major element content data of Xujiahe Formation mud shale.

Sample Number	Depth (m)	LOI (%)	SiO_2 (%)	K_2O (%)	Na_2O (%)	CaO (%)	MgO (%)	Al_2O_3 (%)	TFe_2O_3 (%)	MnO (%)	TiO_2 (%)	P_2O_5 (%)
1	67.4	5.37	80.70	1.62	0.11	0.11	0.43	14.82	0.85	0.04	1.14	0.03
2	68.4	4.00	80.61	2.63	0.12	0.17	0.60	13.34	1.43	0.01	0.89	0.05
3	93.9	6.64	73.95	2.42	0.12	0.06	0.54	16.97	4.87	0.04	0.80	0.07
4	129.6	8.04	68.87	3.26	0.15	0.09	0.91	18.99	6.27	0.02	1.18	0.07
5	130.4	5.30	78.99	2.52	0.12	0.08	0.59	15.57	0.90	0.02	0.99	0.07
6	145.8	4.22	82.62	1.55	0.10	0.11	0.72	9.52	4.51	0.02	0.63	0.09
7	147.5	7.75	66.37	3.99	0.15	0.10	1.76	19.04	7.18	0.04	1.05	0.13
8	307.9	6.73	70.89	3.58	0.36	0.14	1.68	16.61	5.54	0.03	0.85	0.13
9	308.6	6.32	73.19	3.28	0.42	0.12	1.35	14.62	5.92	0.05	0.69	0.19
10	310.2	6.42	65.32	4.12	0.17	0.34	2.51	18.48	7.56	0.19	0.91	0.19
11	311.6	7.53	67.79	4.30	0.20	0.07	2.11	19.47	4.77	0.03	0.93	0.07
12	324.7	8.32	64.60	4.36	0.15	0.59	1.90	20.44	6.54	0.08	0.95	0.20
13	326.1	9.43	58.78	5.25	0.17	0.08	1.44	24.98	7.99	0.01	1.00	0.09
14	326.7	15.28	64.92	5.05	0.17	0.32	1.40	24.55	2.32	0.01	0.99	0.03
15	391.0	17.03	50.66	2.05	0.15	0.16	1.10	30.01	14.78	0.03	0.80	0.07
16	446.2	5.83	74.03	4.39	0.16	0.14	0.87	17.70	1.64	0.02	0.84	0.03
17	453.0	7.03	64.12	6.02	0.18	0.22	1.35	23.23	3.44	0.03	1.05	0.10
18	495.5	18.09	53.26	3.68	0.16	17.68	4.40	14.34	5.20	0.22	0.71	0.18
19	495.8	15.15	58.19	3.73	0.18	12.18	4.38	14.97	5.08	0.20	0.72	0.22

Table 1. *Cont.*

Sample Number	Depth (m)	LOI (%)	SiO_2 (%)	K_2O (%)	Na_2O (%)	CaO (%)	MgO (%)	Al_2O_3 (%)	TFe_2O_3 (%)	MnO (%)	TiO_2 (%)	P_2O_5 (%)
20	496.3	19.49	48.25	3.67	0.15	22.22	4.38	14.52	5.41	0.30	0.69	0.25
21	497.6	9.90	65.54	3.56	0.45	4.96	3.64	14.42	6.02	0.23	0.76	0.22
22	499.9	3.52	76.06	3.32	1.02	0.36	1.36	12.14	4.91	0.04	0.47	0.17
23	517.0	5.92	73.05	4.79	0.16	0.15	1.28	17.64	1.84	0.01	0.87	0.03
24	517.8	7.12	65.70	4.84	0.16	0.41	2.57	19.08	5.82	0.03	0.94	0.23
25	518.5	7.68	67.57	3.98	0.20	2.07	3.31	15.51	6.08	0.09	0.79	0.19
26	525.3	5.55	73.28	3.53	0.56	0.49	1.44	13.91	5.59	0.03	0.68	0.27
27	552.5	4.18	81.44	2.86	0.12	0.09	0.91	10.92	2.76	0.03	0.68	0.05
28	564.2	4.82	78.97	3.02	0.13	0.11	1.34	11.72	3.67	0.03	0.71	0.09
29	565.3	5.52	77.32	3.24	0.14	0.13	1.33	13.07	3.69	0.02	0.78	0.10
30	567.1	6.28	71.38	4.74	0.14	0.11	1.56	17.66	2.96	0.03	1.15	0.06

4.3.2. Trace Element Geochemistry

The most abundant trace elements in the sample were Ba (466 ppm), Zr (313 ppm), Rb (141 ppm), and V (105 ppm). This was followed by Ce (94 ppm), Sr (83 ppm), Zn (71 ppm), Cr (67 ppm), Li (63 ppm), and La (54 ppm). The general content of other trace elements is less than 50 ppm. The trace elemental compositions of the Xujiahe Fm from the Xindianzi section in Sichuan Basin are shown in Table 2.

Table 2. Trace element content data of Xujiahe Formation mud shale.

Sample Number	Depth (m)	V (ppm)	Cr (ppm)	Sr (ppm)	Ba (ppm)	U (ppm)	Th (ppm)	Ni (ppm)	Co (ppm)	Cu (ppm)
1	67.4	132.61	74.21	81.51	234.54	4.59	19.89	29.35	9.66	28.63
2	68.4	82.49	50.66	82.84	444.34	3.76	15.45	24.04	10.41	16.14
3	93.9	75.46	48.85	92.40	856.91	3.63	14.85	25.13	10.56	14.12
4	129.6	68.50	47.49	65.37	353.82	3.46	14.21	18.33	6.16	13.17
5	130.4	77.18	57.93	79.28	863.55	3.21	15.88	24.94	11.21	12.31
6	145.8	97.23	67.08	77.17	565.21	3.13	16.24	29.76	12.28	22.05
7	147.5	126.90	78.12	78.25	559.49	3.92	18.95	34.82	19.04	35.73
8	307.9	98.86	51.42	66.82	567.52	3.54	15.32	14.81	6.13	41.51
9	308.6	52.91	45.34	82.98	563.64	1.95	10.33	29.23	12.61	11.23
10	310.2	89.82	53.42	91.63	475.76	2.90	13.29	26.82	12.89	20.99
11	311.6	86.84	43.27	204.39	313.02	2.84	9.89	29.79	11.79	25.01
12	324.7	91.42	43.90	124.48	343.83	3.09	10.15	29.44	11.38	24.54
13	326.1	97.80	46.60	194.43	351.02	3.08	10.80	28.74	10.39	27.72
14	326.7	163.85	80.99	145.49	674.12	4.07	19.74	11.57	5.38	8.34
15	391	99.17	50.67	81.23	541.93	3.50	17.68	10.50	1.84	10.51
16	446.2	170.38	121.50	40.33	313.68	4.69	26.89	34.14	15.91	20.21
17	453	152.34	58.70	71.24	427.09	5.92	15.30	52.73	8.93	58.80
18	495.5	150.65	102.39	74.46	444.56	4.85	21.87	37.62	9.94	45.37
19	495.8	115.53	84.40	67.29	398.31	3.66	16.87	30.45	11.10	32.53
20	496.3	129.90	69.82	78.84	1051.15	4.03	14.91	27.74	10.83	23.61
21	497.6	124.70	87.09	64.98	500.94	3.36	16.30	33.22	12.39	33.42
22	499.9	86.94	58.82	62.50	534.79	2.61	12.21	31.81	11.11	20.14
23	517	93.00	90.97	51.76	515.53	3.36	14.93	42.05	12.38	21.75
24	517.8	128.72	112.03	64.92	380.92	3.73	16.80	46.45	26.45	32.97
25	518.5	57.55	51.85	24.47	181.25	2.17	10.45	31.99	5.96	13.71
26	525.3	85.89	57.30	72.25	288.56	3.27	14.73	19.63	1.76	7.70
27	552.5	132.53	112.63	81.48	388.36	4.27	18.55	21.94	6.60	27.68
28	564.2	104.93	70.61	51.09	306.19	2.74	13.43	17.30	17.06	8.83
29	565.3	89.22	48.19	61.78	272.90	3.16	13.23	9.82	2.01	7.05
30	567.1	100.77	52.81	42.93	290.25	3.12	16.41	11.30	14.77	6.95

4.4. Type of Organic Matter

Both outcrops and underground cuttings of Xujiahe Fm throughout the research site are constituted of alternating grayish black shale and dark mudstone. Three dark mudstone samples and three gray–black shale samples are selected for kerogen maceral analysis, and TI index is calculated based on the content of each maceral. According to the TI index criterion, kerogen is type I when TI $\geq$ 80; when 40 < TI < 80, kerogen is II_1 type; when 0 < TI < 40, kerogen is II_2 type; when TI < 0, it is type III [50,51]. The kerogen maceral data of gray–black shale and dark mudstone in Xujiahe Fm Mbr 1 are shown in Table 3.

Table 3. Maceral group of Member 1 of Xujiahe Formation in Xinduan section.

No.	Lithology	Sapropelite Group		Exinite Group						Vitrinite Group	Inertinite Group	TI	Type
		Planktonic Alga	Sapropelic Amorphous	Resinite	Cork	Cutinite	Spore Powder	Mycosporite	Humus Amorphous	Vitrinite	Fusinite		
1	Gray–black shale		0.48			0.24	0.11		0.19	0.61		29.25	II_2
2	Gray–black shale		0.32			0.26			0.22	0.65		7.25	II_2
3	Gray–black shale		0.35			0.05			0.38	0.72		2.5	II_2
4	Dark mudstone		0.87			0.25	0.3		0.33	2.4	0.1	–59	III
5	Dark mudstone		0.34			0.46			0.4	1.63		–45.25	III
6	Dark mudstone		0.32			0.51			0.72	2.17		–69.25	III

The results of the TI type index of kerogen are as follows: the proportion of sapropelite group and exinite group in the dark mudstone of Xujiahe Fm Mbr 1 is relatively low, while the proportion of vitrinite group is relatively high, and The TI values are all less than 0, indicating that kerogen is type III. The proportion of sapropelite group and exinite group in the gray–black shale of Xujiahe Fm Mbr 1 is higher, while the proportion of vitrinite group is lower, and the TI value is between 0 and 30, indicating II_2 kerogen (Table 3). Type III kerogen is predominantly sourced from continental plant matter with significant content of lignin [52], cellulose and tannin, while type II_2 kerogen is mainly derived from a mixture of marine plankton, plant and microbial organic matter [53,54]. The results indicate that the southeast of Sichuan Basin may have been repeatedly submerged or affected by sea water during the sedimentation period.

5. Discussion

5.1. Evidence of Marine–Continental Transitional Shales

5.1.1. Indicator of Sedimentary Structure

The lower section of the Xujiahe Formation in the southeastern Sichuan Basin contains various sedimentary structures. Among them, Submember 1 of Member 1 primarily exhibits continental sedimentary structures. These sedimentary structures include the following: (1) Lenticular sandbody (Figure 4c), often formed in delta plain distributary channels, with sedimentary characteristics like riverbed deposits in rivers [55]. (2) A dual structure (Figure 4d), also common in delta plain distributary channels, usually appears as fine-grained sediment overlaying bed sediments composed of coarse sand and gravel [56,57].

Submember 2 of Member 1 in the Xujiahe Formation primarily exhibits marine–continental transitional sedimentary structures. Typical sedimentary structures include the following: (1) Positive rhythmic stratification with upward decreasing in grain size and upward decreasing in bedding scale (Figures 4a and 5b). This rhythmic repetition is caused by regular alternating changes in material transport or production modes. These changes are usually caused by the tidal rhythm formed by the subenvironmental changes in the ocean tidal zone [58] or the seasonal rhythm formed by the seasonal changes in the climate [59]. (2) Bioturbated structures and boreholes (Figure 4e), where bioturbation is primarily characterized by high-angle inclined boreholes, burrows, and fodinichnion, typically found in mudflats with weaker water currents. Vertical borehole organisms are almost exclusively bottom-dwelling filter feeders that feed on suspended particles, indicating an ecological environment is the lower intertidal zone to the subtidal zone with moderate to relatively high hydrodynamic conditions [60,61]. (3) Vein bedding (Figure 5a,e), wavy bedding (Figure 5a,e), and lenticular bedding (Figure 5a,d), which are commonly observed in delta interdistributary environments with lack of source input, including mud flats, mixed

flats, and tidal channels [62,63]. (4) Swash cross-bedding is characterized by multiple sets of cross-stratification where the upper cross–beds truncate the lower ones. This phenomenon is commonly observed in tidal sand bars [64,65]. (5) Double mud-drape structure (Figure 5a,d) and feathery cross-bedding (Figure 5d). The double mud-drape structure and feathery cross-bedding typically develop in tidal-influenced delta front subaqueous distributary channels. These features are commonly modified by tidal bidirectional flow and have strong hydrodynamic conditions and distinct bidirectional flow characteristics [66,67]. (6) Soft sedimentary deformation structures (Figure 5e) are relatively common in core observation, generally exist in silty sand and argillaceous siltstone, and can appear in delta front and deep-water gravity flow deposits [63,68].

These sedimentary structures reflect that SubMbr 1 of Mbr 1 from the Xujiahe Fm stage in southeastern Sichuan was a delta sedimentary system with a high quantity of terrigenous clastic sediments carried by rivers. In SubMbr 2 of Mbr 1 from the Xujiahe Fm stage, the area was influenced by tidal action, which was reflected in the symbiosis of sedimentary structures formed by current action and wave action.

5.1.2. Indicator of Biological Evolution

The evidence of outcrop fossils and sporopollen fossils indicates that the sediments of Xujiahe Fm Mbr 1 were influenced by both marine and continental influences and can be compared with other sections in the basin, which are considered to be marine–continental transitional facies before.

By comparing the fossils found in two submembers of the Xindianzi section in the southeastern Sichuan Basin, the results show that SubMbr 1 of Mbr 1 from the Xujiahe Fm consists of land plant fossils dominated by gymnosperms and ferns (Figure 6b,c,e), while the land plant fossils in SubMbr 2 of Mbr 1 from the Xujiahe Fm are significantly less. In addition, *Micrhystridium* sp. (Figure 6a), a representative marine fossil, appeared in SubMbr 2 of Mbr 1 from the Xujiahe Fm [23]. Such fossils are found in marine strata both at home and abroad, which are significant for analyzing the depositional environment. By comparing the Xindianzi section in the southeastern Sichuan Basin with the Xuanhan section and Tanba section in the eastern part of the basin, we can see that *Sulcusicystis* sp. appeared in the Xuanhan section (Figure 6d), and marine fossils of Lingula sp. (Figure 6e) were also found in the eastern part of the basin. All these indications indicate that the marine–continental transitional conditions characterized the depositional environment of the early Xujiahe Fm in the southeastern Sichuan Basin.

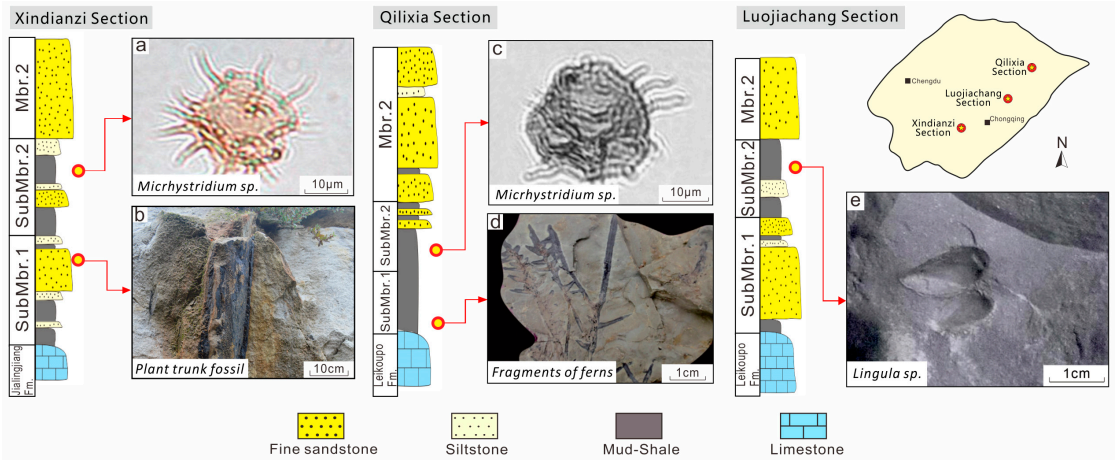


Figure 6. Comparison of outcrop fossils in early Xujiahe Fm, Sichuan Basin. (**a**) *Micrhystridium* sp. from upper part of Xujiahe Fm Mbr 1 in the Xindianzi section, Southeast Sichuan Basin; (**b**) tilted tree

trunk fossil from Xujiahe Fm Mbr 1 in the Xindianzi section, Southeast Sichuan Basin; (**c**) *Micrhystridium* sp. from Xujiahe Fm Mbr 1 in the Qilixia section, Northeast Sichuan Basin; (**d**) fragments of plant fossil from Xujiahe Fm Mbr 1 in the Qilixia section, Northeast Sichuan Basin; [69]; (**e**) *Lingula* sp. from Xujiahe Fm Mbr 1 in the Luojiachang section, East Sichuan Basin [70].

The palynological analysis of 38 mud-shale samples from the Xujiahe Formation reveals that the early sedimentary records exhibit high abundance and diversity of fossils, with good preservation conditions. While the main components in each sample are generally consistent, their percentage content varies.

The Xindianzi section is compared with Tanba section and Qilixia section in the northeastern Sichuan Basin, which are also considered as the marine–continental transitional facies [71]. Among the three sections, the top five abundant components of sporopollen fossil in the Xujiahe Fm are *Dictyophyllidites*, *Concavisporites*, *Osmundacidites*, *Chasmatosporites*, and *Cycadopites*. *Dictyophyllidites* and *Concavisporites* experienced the evolution of abundance from high (SubMbr 1) to low (SubMbr 2) and then rising (Mbr 2) in the Early Xujiahe period. However, *Osmundacidites*, *Chasmatosporites*, and *Cycadopites* experienced a process of change from low (SubMbr 1) to high (SubMbr 2) and then decreased (Mbr 2) (Figure 7). This abundance change is almost consistent with the early variation trend of Xujiahe Fm found in the Qilixia section and Tanba section [72,73]. This indicates that the sedimentary environment of Xujiahe Fm Mbr 1 in the Xindianzi section is generally consistent with that of the Qilixia section and other comparable sections, confirming it as a marine–continental transitional sedimentary environment.

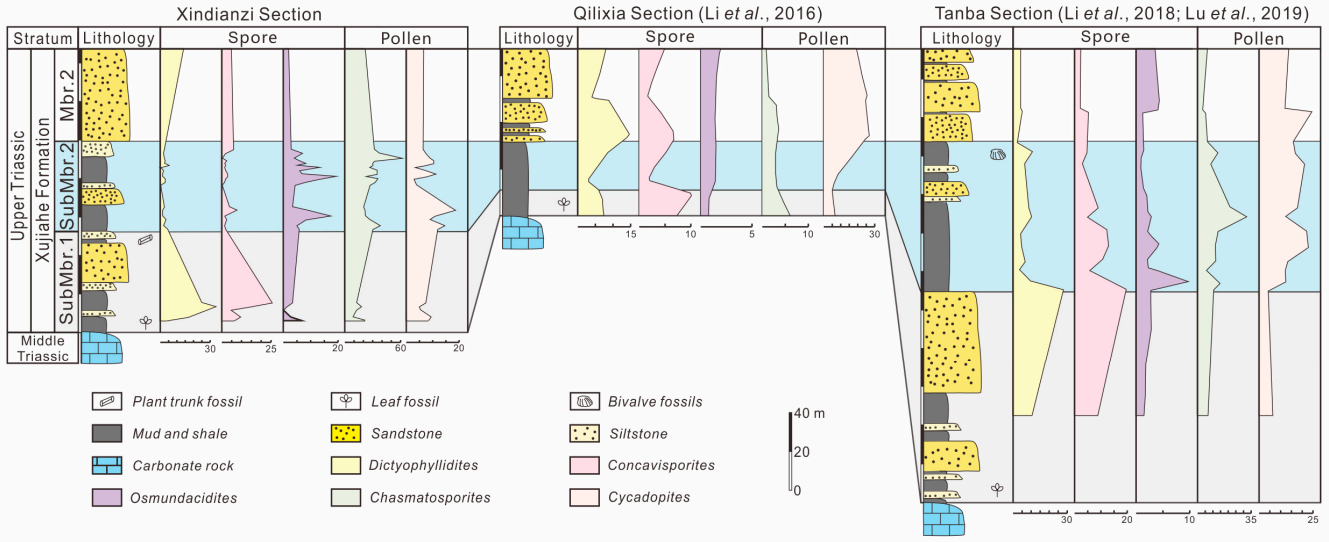


Figure 7. Changes of major Sporopollen genera in abundance from the lower Xujiahe Fm in distinct regions of Sichuan Basin, China (modified from Lu et al., 2023) [23,72–74].

5.1.3. Major and Trace Element Geochemistry

The geochemical composition of sedimentary rocks is influenced by chemical weathering and sedimentary recycling. Parameters such as the Chemical Index of Alteration (CIA), the Index of Compositional Variability (ICV), and the Park Weathering Index (WIP) have been proposed as quantitative indicators for analyzing weathering intensity, sedimentary sorting, and recycling processes.

The CIA values of the samples from Xujiahe Fm Mbr 1 range from 72.13 to 78.84, with an average value of 77.40, indicating moderate chemical weathering. The ICV values of the samples from Xujiahe Fm Mbr 1 range from 0.52 to 1.05, with an average value of 0.84, close to 1.0, suggesting weak sedimentary recycling. In the CIA–ICV plot, most samples fall within the moderate weathering zone (Figure 8a). The CIA–WIP plot indicates

that the Xujiahe Formation experienced moderate chemical weathering and is primarily characterized by first-cycle deposition (Figure 8b).

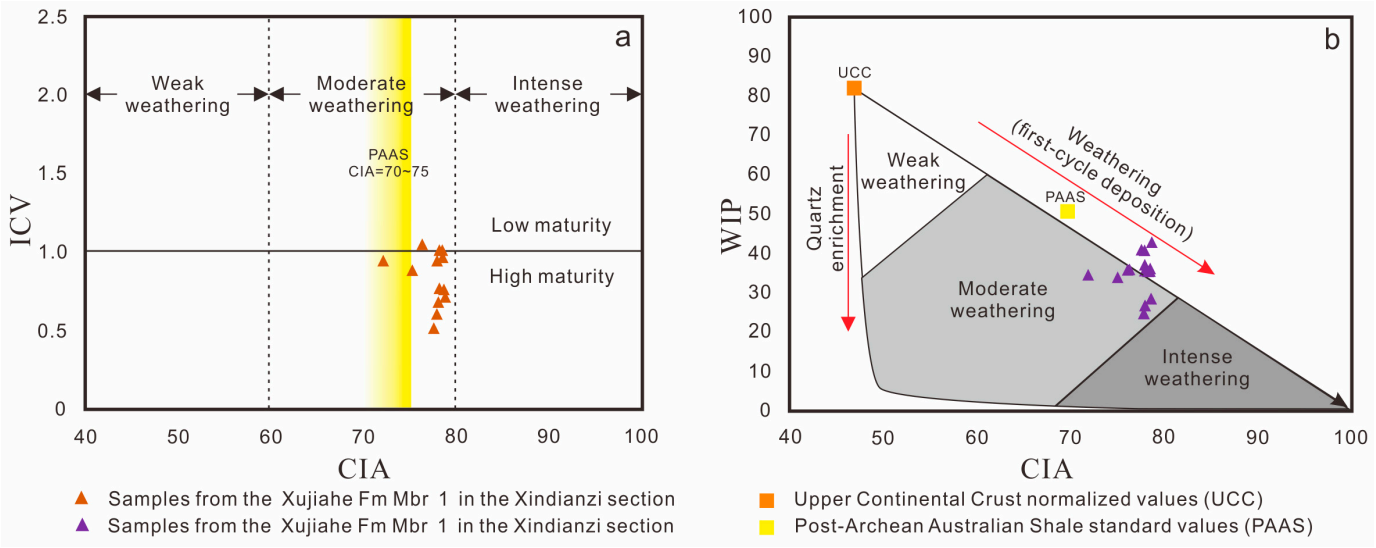


Figure 8. CIA–ICV plot (**a**) and CIA–WIP plot (**b**) for Mbr 1 of the Xujiahe Fm in the southeastern Sichuan Basin.

(1) Paleosalinity

As an important index of paleoenvironment analysis, paleosalinity acts as a key factor in restoring the paleogeographic environment during the sedimentary period. The most used geochemical indices for restoring paleosalinity are Sr and Sr/Ba. With the increase in paleosalinity, Ba elements precipitated in the form of $BaSO_4$ and Sr precipitated in the form of $SrSO_4$, and the content of Sr and value of Sr/Ba had a closely association with the paleosalinity of water. Therefore, the Sr content and Sr/Ba values can illustrate the paleosalinity alterations in geological history. Previous studies believed that Sr < 90 ppm indicates a freshwater environment, Sr content between 90 ppm and 300 ppm demonstrates a brackish water condition, and Sr content > 800 ppm demonstrates a salt water condition. Sr/Ba > 0.8 is brackish water sedimentation; Sr/Ba < 0.5 is freshwater sedimentation; brackish water deposits with Sr/Ba are between 0.5 and 0.8 [75,76]. Based on the examination results of the samples from Xujiahe Fm Mbr 1 of Xindianzi section, the Sr content of SubMbr 1 of Mbr 1 from the Xujiahe Fm is 42.93 ppm–81.48 ppm, with an average of 61.90 ppm; Sr/Ba ranges from 0.09 to 0.35, with an average of 0.18. The Sr concentration of SubMbr 2 of Mbr 1 from the Xujiahe Fm was 24.47 ppm–194.43 ppm, with an average of 91.63 ppm; Sr/Ba ranged from 0.12 to 0.65, with an average of 0.29 (Figure 9). These results indicate that the southeast region of the Sichuan Basin was characterized by a freshwater sedimentary condition during SubMbr 1 of Mbr 1 from the Xujiahe Fm sedimentary period and changed into a brackish water sedimentary environment during SubMbr 2 of Mbr 1 from the Xujiahe Fm sedimentary period.

In addition, the ratio of Mg, Al, Fe, Ca, etc., can also effectively reflect the paleosalinity. Mg is a typical marine element, and Al is a typical terrigenous element. Some scholars proposed that $m = (MgO/Al_2O_3) \times 100$ could be used as a major element index to measure the paleosalinity. They believe that an m value less than 20 demonstrates a freshwater sedimentary condition, an m value higher than 50 indicates a saltwater sedimentary environment, and a brackish water environment between 20 and 50. CaO/(Fe + CaO) is also an indicator of seawater salinity, with a ratio less than 0.2 indicating low salinity, 0.2–0.5 indicating moderate salinity, and greater than 0.5 indicating high salinity [77]. The m values of SubMbr 1 of Mbr 1 from the Xujiahe Fm ranged from 8.35 to 11.42, with

an average of 9.82; CaO/(Fe + CaO) fluctuates between 0.03 and 0.08, with a typical value of 0.04. The m values of SubMbr 2 of Mbr 1 from the Xujiahe Fm ranged from 7.24 to 30.71, with an average of 21.07; CaO/(Fe + CaO) fluctuates between 0.07 and 0.80, with a typical value of 0.40 (Figure 9). The palaeosalinity reflected by them is in line with the Sr and Sr/Ba results, indicating that a continental freshwater depositional setting was present in SubMbr 1 of Mbr 1 from the Xujiahe Fm sedimentary period and that there was a brackish water sedimentary environment in SubMbr 2 of Mbr 1 from the Xujiahe Fm sedimentary period.

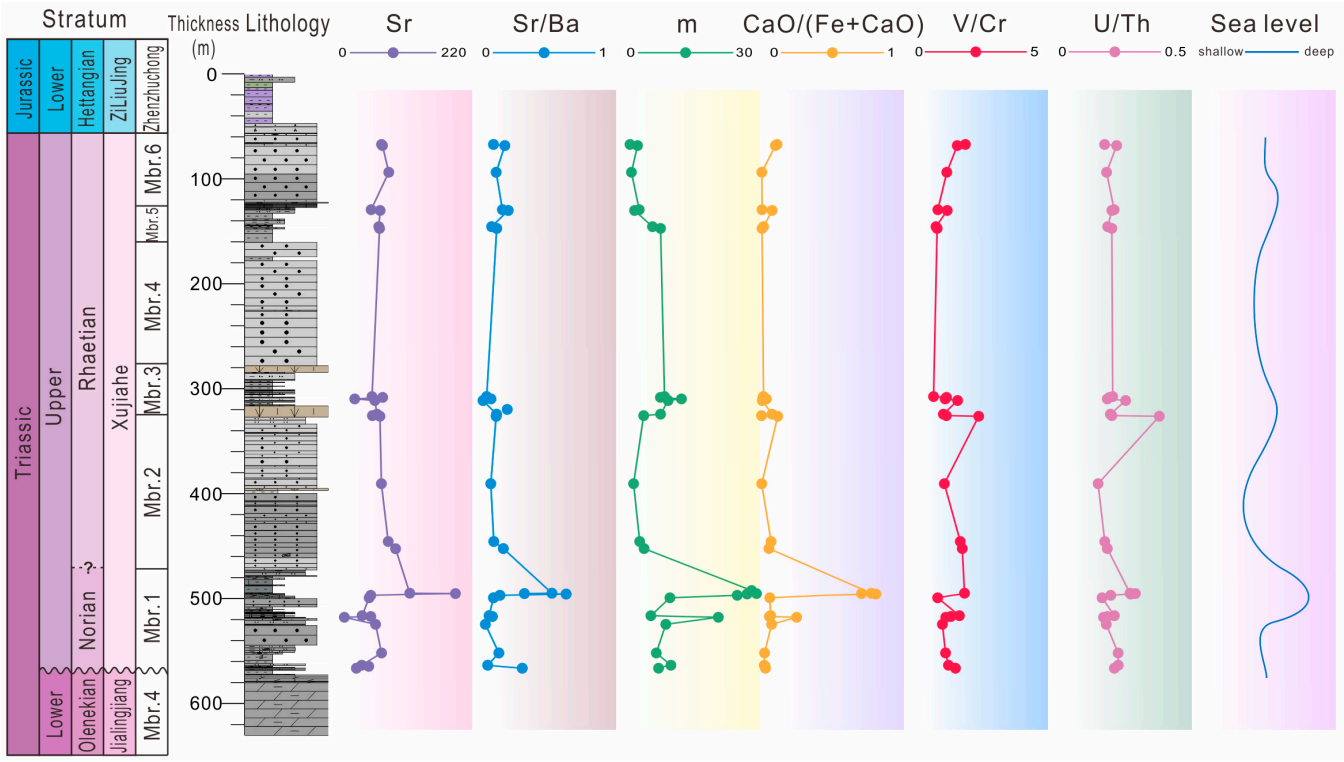


Figure 9. Paleo-salinity, paleo-redox, paleo-climate, and paleo-sea-level changes indicated by the element geochemical indexes of Xujiahe Fm in Xindianzi Section, Southeast Sichuan Basin.

Generally, Sr, Sr/Ba, CaO/(Fe + CaO), and m value indexes all altered dramatically in the period of Xujiahe Fm Mbr 1. The index of SubMbr 1 of Mbr 1 from the Xujiahe Fm is lower than that of SubMbr 2, indicating that a continental freshwater depositional setting was present during SubMbr 1 period, and seawater entered the basin during SubMbr 2 period, transitioning to a marine–continental transitional depositional setting. During SubMbr 2 period, it changed into a continental depositional setting again. The western region of the basin has remained a saltwater marine depositional setting throughout the period of Xujiahe Fm Mbr 1 [78].

(2) Paleo-oxidation–reduction

Water redox conditions vary under different sedimentary environments. Geochemical indexes of V/Cr and U/Th are commonly used to analyze paleo-redox conditions. Cr mainly exists in the form of soluble Cr^{6+} chromate in oxygen-rich water, which is reduced to Cr^{3+} under hypoxia conditions and absorbed into sediments by humus and Fe or Mn hydroxides. The chemical properties of V are similar with Cr, soluble in water under oxidation conditions, and precipitated under reduction conditions. Therefore, V/Cr can be used to restore paleo-oxidation–reduction conditions. V/Cr < 2 demonstrates an oxidation environment, 2 < V/Cr < 4.25 demonstrates an oxygen-poor environment, and V/Cr > 4.25 demonstrates anoxic environment [79]. Th is unaffected by redox conditions, whereas U is soluble in water in oxy-gen-rich environments but easily precipitates in anoxic conditions;

hence, the U/Th ratio can also be applied to determine water redox conditions [80]. The general consensus is that U/Th > 0.5 signifies an anoxic environment, and U/Th < 0.5 represents an oxidizing environment. The V/Cr ratio of SubMbr 1 of Mbr 1 from the Xujiahe Fm in Xindianzi section is 1.33–1.79, with an average of 1.55; the U/Th ratio is 0.20–0.24, with an average of 0.23. The V/Cr ratio of SubMbr 2 is 1.17–2.10, with an average of 1.75; the U/Th ratio is 0.19–0.30, with an average of 0.24 (Figure 9).

The analysis of V/Cr and U/Th shows that the sedimentary environment of Xujiahe Fm Mbr 1 is a weak oxidation environment, and SubMbr 2 stage exhibits weaker oxidation intensity compared to SubMbr 1 stage.

5.1.4. Indicator of Organic Matter Type

Kerogen maceral analysis indicates that SubMbr 1 of Mbr 1 from the Xujiahe Fm stage in the paleouplift of the southeast basin is a continental environment, SubMbr 2 of Mbr 1 from the Xujiahe Fm stage is a marine–continental transitional environment, and the west of the basin has been a marine sedimentary environment. A total of six samples (three dark mudstone samples from SubMbr 1 and three gray–black shale samples from SubMbr 2) were selected for kerogen type analysis by the TI value. The results show that the dark mudstone of SubMbr 1 in the southeastern Sichuan Basin contains type III kerogen, while the gray–black shale of SubMbr 2 contains type II_2 kerogen. In contrast, the kerogen types of Xujiahe Fm Mbr 1 in the western Sichuan Basin are mostly type II_2 [33]. Terrestrial plant organic matter, particularly rich in lignin, cellulose, and tannin, is the primary source of type III kerogen. Type II_2 kerogen is predominantly formed from a blend of marine plankton, plant, and microbial organic matter. The results above confirm that the Luzhou palaeouplift isolated the western sea water, and the uplift region was dominated by continental sedimentation in SubMbr 1 stage. During the SubMbr 2 stage, the southeast of the basin became a marine–continental transitional sedimentary environment, while the western basin was a marine sedimentary environment.

5.2. Sedimentary Model and Hydrocarbon Potential

The characteristics of "Whole basin covered with sand" in Xujiahe Fm have puzzled scholars for a long time, hindering a unified understanding of its sedimentary environment, and the division of sedimentary facies has been debated. Zheng Rongcai (2004) stated that the western Sichuan Basin is mainly a braided river delta–lake swamp facies [81]. Lin Liangbiao (2006) suggested that the western part of the Sichuan Basin was dominated by marine or marine–continental transitional facies [82]. Wang Liangjun (2005) stated that the Xujiahe Fm in Chishui area, the southern margin of the Sichuan Basin, is a meandering river-braided river-flood plain sedimentation [83]. Zeng Wei (2006) proposed that the Xujiahe Fm in the southern Sichuan Basin is a braided river-delta-lacustrine swamp facies [84]. Jiang Zaixing (2007) stated that the southeastern Sichuan Basin is a meandering river delta sedimentation [85]. Gao Zhiyong (2007) argued that the first, third, fifth, and sixth members of the Xujiahe Fm in the Central Sichuan Basin are meandering river sedimentation, while the second and fourth members are braided river sedimentation [86]. Liu Jinhua (2007) put forward the views of "marine sedimentation in early stage" and "continental sedimentation in late stage" based on the study of sequence stratigraphy [87]. Hou Fanghao and Jiang Yuqiang (2005) held that the sandstones of the Xujiahe Fm in the central and southern Sichuan Basin were mainly formed in beach bar of shallow lake [88]. Zhao Xiafei (2008) stated that the Xujiahe Fm in the Anyue area of Central Sichuan Basin is an offshore tidal sedimentation [89]. Lai Wei (2019) suggested that the northeastern part of the Sichuan Basin was also dominated by marine–continental transitional facies during the early stage of the Xujiahe Formation [90].

Building upon previous research findings and integrating the results of this study, the sedimentary model of the marine–continental transitional shale of the Upper Triassic Xujiahe Fm Mbr 1 in the southeastern Sichuan Basin is established: During SubMbr 1 of Mbr 1 from the Xujiahe Fm period, from the western to the eastern region, the Sichuan Basin progressively transitioned from the offshore lacustrine system to the near-source delta system (Figure 10a). During the Xujiahe Fm sedimentary period, two primary sources had a major impact on the southeastern Sichuan Basin: The Kangdian–Qianzhong palaeoland and the Jiangnan–Xuefengshan palaeouplift. The braided water system formed by these two source direction systems is interwoven here. As the lake basin contracted, abundant sediment supply allowed sand bodies to advance into the lake, resulting in a reverse rhythm between the pre-delta mud zone and the delta front zone. In SubMbr 2 of Mbr 1 from the Xujiahe Fm sedimentary period, the sea level rose, and the sea water gradually advanced to the land and submerged the Luzhou palaeo-uplift, which showed an obvious positive rhythm of the pre-delta mud belt. In this period, the southeast of the Sichuan Basin transitioned from continental sedimentation to marine–continental transitional sedimentation, while the west part of basin was marine sedimentation (Figure 10b). Utilizing field observations and drilling data, combining previous research, it is identified that southeast of the Sichuan Basin comprised a shallow water braided river delta sedimentary system in Xujiahe Fm Mbr 1 while influenced by tidal forces during transgression periods.

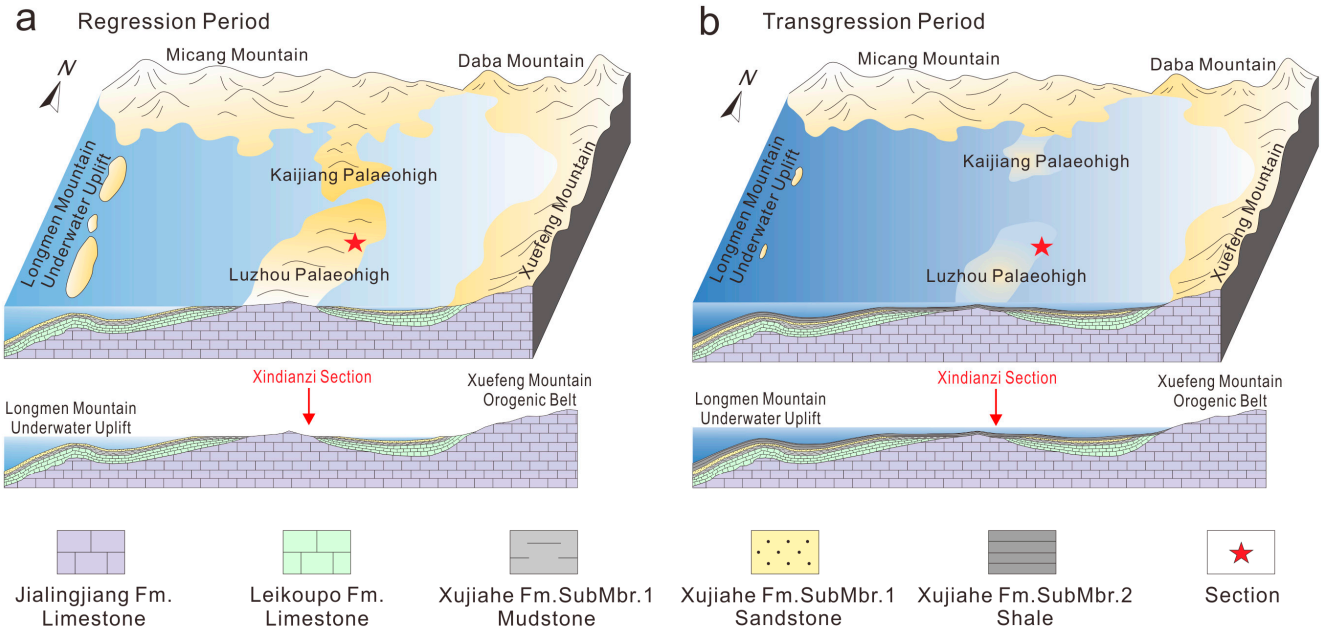


Figure 10. Sedimentary model of the first member of Xujiahe Fm, Southeast Sichuan Basin. (**a**) Regression period. (**b**) Transgression period.

According to previous studies, the higher the abundance of organic matter, the greater the gas generation potential of shale [91]. Moreover, the adsorption of shale gas on organic matter surfaces is influenced by TOC, with higher TOC leading to increased adsorption under specific pressure conditions.

The TOC of Xujiahe Fm mud shale in the southeastern Sichuan Basin ranges from 0.95% to 7.59%, with an average of 2.53%. Among them, the TOC of Xujiahe Fm Mbr 1 ranges from 1.2 to 7.34%, with an average of 3.2%. The TOC of Xujiahe Fm Mbr 3 ranges from 0.99 to 6.22%, with an average of 2.6%. The TOC of Xujiahe Fm Mbr 5 ranges from 0.95% to 1.61%, with an average of 1.2%. The Ordos Basin has reached a mature phase in the exploration and development of shale gas in marine–continental transitional environments. The average

TOC of Taiyuan Formation, Benxi Formation, and Shanxi Formation is 3.0%, 4.1%, and 2.7%, respectively [4]. Compared with the Ordos Basin, the average TOC of Xujiahe Fm in the southeastern Sichuan Basin is slightly lower, but the average TOC of Xujiahe Fm Mbr 1 is slightly higher than that of the Benxi Formation and comparable to the Shanxi Formation. According to the "Criteria for Selecting Favorable Areas for marine–continental transitional Shale Gas" issued by the Oil and Gas Resources Strategy Center of the Ministry of Land and Resources of China, the lower limit of shale gas producing is TOC > 1.5%, and the standard for favorable gas producing shale is TOC > 2.0%. The outcomes reveal that the Xujiahe Fm's marine–continental transitional shale in the southeastern Sichuan Basin exhibits a high content of organic material, part of layers meeting the criteria for favorable gas-producing shale.

6. Conclusions

(1) Field observations in the study area have revealed depositional structures indicative of a transitional environment, including tidal rhythmites, double mud-drape structures, and feather cross-bedding. In Xujiahe Fm Mbr 1, the abundance of sporopollen fossils and land plant fossils both decreased significantly from bottom to top. These observations, along with other evidence, suggest that in SubMbr 2 of Mbr 1 from the Xujiahe Fm stage in Late Triassic in the southeastern Sichuan Basin, the sedimentary environment was characterized by a marine–continental transition.

(2) Geochemical element indicators further confirm the marine–continental transitional nature in the southeastern Sichuan Basin during the stage of SubMbr 2 of Mbr 1 from the Xujiahe Fm in Late Triassic. The Sr content, Sr/Ba ratio, m value, and CaO/(Fe + CaO) ratio all point to a brackish water environment. The V/Cr and U/Th ratios indicate weakly oxidizing conditions. Additionally, the TI values suggest that the organic matter type is predominantly type II_2–III, consistent with characteristics of marine–continental transitional facies.

(3) The shallow-water braided river delta sedimentary system of in Mbr 1 of the Xujiahe Fm, southeastern Sichuan Basin, was influenced by tides during the transgression period. During SubMbr 1 of Mbr 1 from the Xujiahe Fm stage, this system exhibited near-source deltaic sedimentation under continental conditions, characterized by a shrinking lake basin, abundant material supply, and advancing sand bodies into the lake. Vertically, the pre-delta mud zone and delta front zone display an inverse rhythm. By SubMbr 2 of Mbr 1 from the Xujiahe Fm stage, seawater had crossed the Luzhou paleouplift and connected with the lake basin, transforming the southeastern part of the Sichuan Basin into a marine–continental transitional sedimentary environment. Vertically, the pre-delta mud zone of SubMbr 2 of Mbr 1 from the Xujiahe Fm stage shows a positive rhythm.

(4) In the southeastern Sichuan Basin, the Upper Triassic Xujiahe Fm demonstrates notable organic matter richness and robust potential for hydrocarbon generation. Its TOC content is comparable to that of the Shanxi Fm in the Ordos Basin, a formation renowned for its mature marine–continental transitional shale gas exploitation. The Xujiahe Fm meets the criteria for favorable gas-producing shale, indicating significant potential for shale gas exploration and development. The methodologies and processes utilized in identifying marine–continental transitional shales within the Xujiahe Fm can be applied to analogous formations across various geological periods. As exploration efforts intensify, it is anticipated that shale gas exploitation will expand into new regions.

Author Contributions: Conceptualization, T.Z. and H.H.; methodology, X.Z.; software, L.G. and Y.L.; validation, H.H. and T.Z.; formal analysis, J.Z. and X.Z.; investigation, L.G.; resources, T.Z.; data curation, H.H. and X.Z.; writing—original draft preparation, H.H. and X.Z.; writing—review and editing, T.Z. and J.Z.; visualization, X.Z. and Y.L.; supervision, Y.L.; project administration, T.Z.

and X.Z.; funding acquisition, T.Z. All authors have read and agreed to the published version of the manuscript.

Funding: This research was funded by the National Natural Science Foundation of China (Grant No. 41972120).

Data Availability Statement: The original data can be obtained from the corresponding authors.

Acknowledgments: We extend our sincere appreciation to Tenghui Lu, Jianli Zeng, and Shixin Li for their collaborative efforts in conducting fieldwork and collecting samples from the Yongchuan Section. Additionally, we are deeply grateful to Ying Nie and Fei Lin for their insightful discussions and contributions.

Conflicts of Interest: The authors declare no conflicts of interest.

Abbreviations

The following abbreviations are used in this manuscript:

Fm	Formation
Mbr	Member
SubMbr	Submember
TOC	Total organic carbon

References

1. Ma, Y.S.; Cai, X.Y.; Zhao, P.R. China's shale gas exploration and development: Understanding and practice. *Pet. Explor. Dev.* **2018**, *45*, 589–603.
2. Luo, Q.Y.; Xiao, Z.H.; Dong, C.Y.; Ye, X.Z.; Li, H.J.; Zhang, Y.; Ma, Y.; Ma, L.; Xu, Y.H. The geochemical characteristics and gas potential of the Longtan formation in the eastern Sichuan Basin, China. *J. Pet. Sci. Eng.* **2019**, *179*, 1102–1113.
3. Wang, F.T.; Guo, S.B. Shale gas content evolution in the Ordos Basin. *Int. J. Coal Geol.* **2019**, *211*, 103231.
4. Nie, H.K.; Chen, Q.; Li, P.; Dang, W.; Zhang, J.C. Shale gas potential of Ordovician marine Pingliang shale and Carboniferous–Permian transitional Taiyuan–Shanxi shales in the Ordos Basin, China. *Aust. J. Earth Sci.* **2023**, *70*, 411–422.
5. Zhou, G.X.; Wei, G.Q.; Hu, G.Y. The geochemical and organic petrological characteristics of coal measures of the Xujiahe formation in the Sichuan Basin, China. *Energy Explor. Exploit.* **2019**, *37*, 889–906.
6. Deng, T.; Li, Y.; Wang, Z.J.; Yu, Q.; Dong, S.L.; Yan, L.; Hu, W.C.; Chen, B. Geochemical characteristics and organic matter enrichment mechanism of black shale in the Upper Triassic Xujiahe Formation in the Sichuan basin: Implications for paleoweathering, provenance and tectonic setting. *Mar. Pet. Geol.* **2019**, *109*, 698–716.
7. Dai, J.X.; Ni, Y.Y.; Zou, C.N.; Tao, S.Z.; Hu, G.Y.; Hu, A.P.; Yang, C.; Tao, X.W. Carbon isotope features of alkane gases in the coal measures of the Xujiahe Formation in the Sichuan Basin and their significance to gas–source correlation. *Oil Gas Geol.* **2009**, *30*, 519–529. (In Chinese with English Abstract)
8. Luo, L.; Jia, D.; Qi, J.F.; Wei, G.Q.; Deng, F. Tectono–sedimentary Evolution of the Late Triassic Xujiahe Formation in the Sichuan Basin. *Acta Geol. Sin.-Engl. Ed.* **2013**, *87*, 1554–1568.
9. Tan, X.C.; Xia, Q.S.; Chen, J.S.; Li, L.; Liu, H.; Luo, B.; Xia, J.W.; Yang, J.J. Basin–Scale Sand Deposition in the Upper Triassic Xujiahe Formation of the Sichuan Basin, Southwest China: Sedimentary Framework and Conceptual Model. *J. Earth Sci.* **2013**, *24*, 89–103.
10. Xu, C.M.; Gehenn, J.M.; Zhao, D.H.; Xie, G.Y.; Teng, M.K. The fluvial and lacustrine sedimentary systems and stratigraphic correlation in the Upper Triassic Xujiahe Formation in Sichuan Basin, China. *AAPG Bull.* **2015**, *99*, 2023–2041.
11. Lai, J.; Wang, G.W.; Fan, Z.Y.; Chen, J.; Wang, S.C.; Fan, X.Q. Sedimentary characterization of a braided delta using well logs: The Upper Triassic Xujiahe Formation in Central Sichuan Basin, China. *J. Pet. Sci. Eng.* **2017**, *154*, 172–193.
12. Gou, M.X.; Lu, G.; Deng, B.; Wang, C.C.; Li, Z.W.; Yu, Y.; Yang, R.J.; Jin, X. Tectonic–paleogeographic evolution of the Late Triassic in the Sichuan basin, SW China: Constraints from sedimentary facies and provenance analysis of the Xujiahe Formation. *Mar. Pet. Geol.* **2024**, *160*, 106649.
13. Peng, Y.; Zheng, M.P.; Zhang, Y.S.; Xing, E.Y.; Gui, B.L.; Zuo, F.F. Geochronology and geochemistry of lithium–rich tuffs in the Sichuan basin, western Yangtze: Implication for the magmatic origin and final closure of eastern Paleo–Tethys. *Geosci. Fronti.* **2023**, *14*, 101480.
14. Liu, X.W.; Jiang, F.J.; Zheng, X.W.; Gao, Y.; Zhou, S.Y. Sedimentary Record of the Bio–Geological Events in Tethys: Insight from the Permian Yangtze Block Breakup in the Sichuan Basin. *Appl. Sci.* **2024**, *14*, 11863. [CrossRef]

15. Jian, X.; Weislogel, A.; Pullen, A. Triassic Sedimentary Filling and Closure of the Eastern Paleo–Tethys Ocean: New Insights from Detrital Zircon Geochronology of Songpan–Ganzi, Yidun, and West Qinling Flysch in Eastern Tibet. *Tectonics* **2019**, *38*, 767–787.
16. Meng, L.F.; Chen, W.; Shen, T.; Cai, J.F. A Study on the Provenance of Early to Late Triassic Clastic Rocks From the Northwestern Sichuan Basin, Southwestern China: Constraints on the Early Mesozoic Tectonic Evolution of the Western Yangtze Block. *Fronti. Earth Sci.* **2022**, *10*, 940301.
17. Li, Y.Q.; Li, S.J.; He, D.F.; Gao, J.; Wang, Y.C.; Huang, H.Y.; Zhang, J.T.; Zhang, Y. Middle Triassic tectono–sedimentary development of Sichuan Basin: Insights into the cratonic differentiation. *Geol. J.* **2020**, *56*, 1858–1878.
18. Tang, J.; Wang, J.; Wu, G.H.; Wen, Y.Y.; Nance, R.D.; He, B.; Li, C.H.; Zou, Y. Retreating subduction–related intracratonic rifting in the Ediacaran Sichuan Basin (SW China). *Precambrian Res.* **2024**, *413*, 107569.
19. Yan, Z.K.; Tian, Y.T.; Li, R.; Vermeesch, P.; Sun, X.L.; Li, Y.; Rittner, M.; Carter, A.; Shao, C.J.; Huang, H.; et al. Late Triassic tectonic inversion in the upper Yangtze Block: Insights from detrital zircon U–Pb geochronology from south–western Sichuan Basin. *Basin Res.* **2019**, *31*, 92–113.
20. Li, Z.Q.; Ying, D.L.; Li, H.K.; Yang, G.; Zeng, Q.; Guo, X.Y.; Chen, X. Evolution of the western Sichuan basin and its superimposed characteristics, China. *Acta Petrol. Sin.* **2011**, *27*, 2362–2370.
21. Bo, S.S.; Tian, J.X.; Wang, Y.T.; Fu, S.; Chen, H.C.; Sun, G.Q. Sedimentary environment evolution of marine–continental transitional facies in Xujiahe Formation, northeastern Sichuan Basin: Evidence from element geochemistry. *NGGS* **2024**, *35*, 645–660, (In Chinese with English Abstract).
22. Blakey, R. ~200 Ma Base Map. Colorado Plateau Geosystem Inc. Available online: http://deeptimemaps.com/ (accessed on 6 October 2022).
23. Lu, T.H.; Zhang, X.; Zhang, T.S.; Cheng, Q.S.; He, F.Y.; Zeng, J.L.; Popa, M.E.; Huang, H.; Li, S.X.; Ma, Z.H.; et al. The influence of the Luzhou paleo–uplift in the southeast of the Sichuan Basin on the development of the Upper Triassic Xujiahe Formation. *J. Stratigr.* **2023**, *47*, 176–190, (In Chinese with English Abstract).
24. Mei, M.X.; Liu, S.F. The Late Triassic Sequence–Stratigraphic Framework of the Upper Yangtze Region, South China. *Acta Geol. Sin. Engl. Ed.* **2017**, *91*, 51–75.
25. Li, Y.J.; Shao, L.Y.; Eriksson, K.A.; Tong, X.; Gao, C.X.; Chen, Z.S. Linked sequence stratigraphy and tectonics in the Sichuan continental foreland basin, Upper Triassic Xujiahe Formation, southwest China. *J. Asian Earth Sci.* **2014**, *88*, 116–136.
26. Liu, S.G.; Yang, Y.; Deng, B.; Zhong, Y.; Wen, L.; Sun, W.; Li, Z.W.; Jansa, L.; Li, J.X.; Song, J.M.; et al. Tectonic evolution of the Sichuan Basin, Southwest China. *Earth-Sci. Rev.* **2021**, *213*, 103470.
27. Shu, H.L.; He, F.Y.; Li, J.L.; Zhang, J.H.; Li, M.L.; Rui, Y.; Zou, C.; Yao, Q.C.; Mei, J.; Li, Y.J. Geological characteristics and favorable exploration areas of Wufeng Formation–Longmaxi Formation deep shale in the Da'an Block, Sichuan Basin. *Nat. Gas Ind.* **2023**, *43*, 30–43. (In Chinese with English Abstract)
28. Xu, M.L.; Yang, Y.B.; Sun, C.Y.; Qiu, G.E.; Chen, L.; Jing, L. Geophysical Characterisation and Oil–Gas Resource Analysis of the Southern Huaying Mountain Fault Zone, Sichuan Basin, China. *Minerals* **2023**, *13*, 270. [CrossRef]
29. Tang, L.J.; Yang, K.M.; Jin, W.Z.; Wan, G.M.; Lü, Z.Z.; Yu, Y.X. Differential Tectonic Deformation of the Longmen Mountain Thrust Belt, Western Sichuan Basin, China. *Acta Geol. Sin.-Engl. Ed.* **2009**, *83*, 158–169.
30. Zhang, Y.; Jia, D.; Shen, L.; Yin, H.W.; Chen, Z.X.; Li, H.B.; Li, Z.G.; Sun, C. Provenance of detrital zircons in the Late Triassic Sichuan foreland basin: Constraints on the evolution of the Qinling Orogen and Longmen Shan thrust–fold belt in central China. *Int. Geol. Rev.* **2015**, *57*, 1806–1824.
31. Mu, H.X.; Yan, D.P.; Qiu, L.; Yang, W.X.; Kong, R.Y.; Gong, L.X.; Li, S.B. Formation of the Late Triassic western Sichuan foreland basin of the Qinling Orogenic Belt, SW China: Sedimentary and geochronological constraints from the Xujiahe Formation. *J. Asian Earth Sci.* **2019**, *183*, 103938.
32. Chen, H.L.; Zhu, M.; Chen, S.Q.; Xiao, A.C.; Jia, D.; Yang, G. Basin–orogen patterns and the late Triassic foreland basin conversion process in the western Yangtze Block, China. *J. Asian Earth Sci.* **2020**, *194*, 104311.
33. Wang, Z.H.; Hao, C.G.; Jin, H.; Cun, J.F.; Wu, X.Q.; Bo, D.M.; Su, Y.Q. Geochemical characteristics and hydrocarbon generation potential of main source rocks in the Upper Triassic Xujiahe Formation, Sichuan Basin, China. *Fronti. Earth Sci.* **2023**, *11*, 1233959.
34. Zhang, M.; Huang, G.H.; Li, H.B.; Hu, G.Y.; Zhang, S.C. Molecular geochemical characteristics of gas source rocks from the Upper Triassic Xujiahe Formation indicate transgression events in the Sichuan Basin. *Sci. China-Earth Sci.* **2012**, *55*, 1260–1268.
35. Zhang, X.; Zhao, X.M.; Ge, J.W.; Li, S.X.; Zhang, T.S. Karst topography paces the deposition of lower Permian, organic–rich, marine–continental transitional shales in the southeastern Ordos Basin, northwestern China. *AAPG Bull.* **2024**, *108*, 849–875.
36. *SY/T 5915–2018*; Analysis and Identification for Fossil Spore and Pollen. Petroleum Industry Press: Beijing, China, 2018.
37. *DZ/T 0279.2-2016*; Analysis Methods for Regional Geochemical Sample-Part 2: Determination of Calcium Oxide etc. 27 Elements Content by Inductively Coupled Plasma Optical Emission Spectrometry. Standards Press of China: Beijing, China, 2016.
38. *GB/T3286 (1–9)–2014*; Methods for Chemical Analysis of Limestone and Dolomite—Part 1–9: The Determination of Iron Oxide Content—The o-Phenanthroline Spectrophotometric Method and the Flame Atomic Absorption Spectrometric Method. Standards Press of China: Beijing, China, 2014.

39. *GB/T 14506.28–2010*; Methods for Chemical Analysis of Silicate Rocks—Part 28: Determination of 16 Major and Minor Elements Content. Standards Press of China: Beijing, China, 2010.
40. *DZ/T 0279.3–2016*; Analysis Methods for Regional Geochemical Sample-Part 3: Determination of Barium, Beryllium, Bismuth etc. 15 Elements Content by Inductively Coupled Plasma Mass Spectrometry. Standards Press of China: Beijing, China, 2016.
41. *DZ/T 0279.32–2016*; Analysis Methods for Regional Geochemical Sample-Part 32: Determination of Lanthanum, Cerium etc. 15 Earth Elements Content by Pressurized Acid Digestion-Inductively Coupled Plasma Mass Spectrometry. Standards Press of China: Beijing, China, 2016.
42. *GB/T 19145–2003*; Determination of Total Organic Carbon in Sedimentary Rock. Standards Press of China: Beijing, China, 2003.
43. *SY/T 5125-2014*; Method of Identification Microscopically the Macerals of Kerogen and Indivision the Kerogen Type by Transmitted-Light and Fluorescence. Petroleum Industry Press: Beijing, China, 2014.
44. Shang, Y.K.; Li, Y.M. Sporopollen assemblage of the Upper Triassic in the Mosuo River Valley, Baoding, Sichuan Province. *Acta Palaeontol. Sin.* **1991**, *30*, 334–353, 358–359, 423–426, (In Chinese with English Abstract).
45. Lei, Z.Q. The Sporo–Pollen Assemblage of the Shezhe Formation of Yipinglang Coal Series in Luquan of Yunnan, and Its Stratigraphical Significance. *J. Integr. Plant Biol.* **1978**, *20*, 229—236, 291—292, (In Chinese with English Abstract).
46. Shang, Y.K. Geographical Division of the Late Triassic Pollen Flora in China. *Acta Palaeontol. Sin.* **1998**, *37*, 37–53. (In Chinese with English Abstract)
47. Morbey, J.S. The palynostratigraphy of the Rhaetian stage, Upper Triassic in the Kendelbachgraben, Austria. *Palaeontographica.* **1975**, *B152*, 1–75.
48. Pauli, H.; Gottfried, M.; Dullinger, S.; Abdaladze, O.; Akhalkatsi, M.; Alonso, J.L.B.; Coldea, G.; Dick, J.; Erschbamer, B.; Calzado, R.F.; et al. Recent plant diversity changes on Europe's Mountain summits. *Science* **2012**, *336*, 353–355.
49. Pieńkowski, G.; Niedźwiedzki, G.; Waksmundzka, M. Sedimentological, palynological and geochemical studies of the terrestrial Triassic–Jurassic boundary in northwestern Poland. *Geol. Mag.* **2012**, *149*, 308–332.
50. Wang, Z.W.; Wang, J.; Yu, F.; Fu, X.G.; Chen, W.B.; Zhan, W.Z.; Song, C.Y. Geochemical characteristics of the Upper Triassic black mudstones in the eastern Qiangtang Basin, Tibet: Implications for petroleum potential and depositional environment. *J. Pet. Sci. Eng.* **2021**, *207*, 109180.
51. Zhao, L.Y.; Zhou, P.M.; Lou, Y.; Zhao, Y.Z.; Liu, W.; Liao, Z.W.; Xia, P. Geochemical Characteristics and Sedimentary Environment of the Upper Permian Longtan Coal Series Shale in Western Guizhou Province, South China. *Geofluids* **2021**, *2021*, 9755861.
52. Hakimi, M.H.; Alaug, A.S.; Al Faifi, H.J.; Alramisy, G.A.; Lashin, A.A. Late Jurassic Safer Salt Member in the Al–Jawf sub–basin of NW Sabatayn Basin, Yemen: Geochemical evaluation of organic–rich oil–source rock potential. *Pet. Sci. Technol.* **2019**, *37*, 645–654.
53. Craddock, P.R.; Haecker, A.; Bake, K.D.; Pomerantz, A.E. Universal Curves Describing the Chemical and Physical Evolution of Type II Kerogen during Thermal Maturation. *Energy Fuels* **2020**, *34*, 15217–15233.
54. Du, Y.; Wang, X.Z.; Zhao, R.R.; Chen, C.; Wen, S.Y.; Tang, R.F.; Mo, Q.W.; Zhang, J.Z.; Zhang, Y.; He, S. Controlling factors of organic matter enrichment in continental shale: A case study of the Jurassic Da'anzhai member in the Sichuan Basin. *Fronti. Earth Sci.* **2022**, *10*, 921529.
55. Lou, T.Y.; Feng, C.J.; Sun, M.S.; Chen, Z.Q. The Upper Triassic Braided River Thin–Bedded Tight Sandstone in the Yanchang Formation, Ordos Basin: Sedimentary Characteristics, Seismic Forecasting Method, and Implication. *Processes* **2023**, *11*, 1303. [CrossRef]
56. Ghinassi, M.; Nemec, W.; Aldinucci, M.; Nehyba, S.; Özaksoy, V.; Fidolini, F. Plan–form evolution of ancient meandering rivers reconstructed from longitudinal outcrop sections. *Sedimentology* **2014**, *61*, 952–977.
57. Zhang, L.; Bao, Z.D.; Dou, L.X.; Zang, D.S.; Mao, S.W.; Song, J.; Zhao, J.H.; Wang, Z.C. Sedimentary characteristics and pattern of distributary channels in shallow water deltaic red bed succession: A case from the Late Cretaceous Yaojia formation, southern Songliao Basin, NE China. *J. Pet. Sci. Eng.* **2018**, *171*, 1171–1190.
58. Zeng, Q.L.; Zhang, X.L.; Zhang, R.H.; Zhao, J.L.; Hou, G.F.; Ji, Y.G. Characteristics of tidal action sedimentary system and distribution of favorable sand bodies of Silurian in Tazhong area, Tarim basin, NW China. *Quat. Int.* **2018**, *468A*, 62–71.
59. Zhang, X.L.; Fan, D.J.; Xu, J.P.; Liu, M.; Tian, Y.; Chen, B.; Sun, Z.L.; Liu, W.L.; Yang, Z.S. Sedimentary laminae in muddy inner continental shelf sediments of the East China Sea: Formation and implications for geochronology. *Quat. Int.* **2018**, *464*, 343–351.
60. Flaig, P.P.; Hasiotis, S.T.; Prather, T.J.; Burton, D. Characteristics of a campanian delta deposit controlled by alternating river floods and tides: The loyd sandstone, rangely anticline, Colorado, USA. *J. Sediment. Res.* **2019**, *89*, 1181–1206.
61. Ahmad, W.; Gingras, M.K.; Ranger, M.J.; MacEachern, J.A.; Zonneveld, J.P. Depositional setting and trace fossil suites of the early Cambrian (series 2, stage 4) Khussak Formation, east–central salt range, north–west sub–Himalayas, Pakistan. *Mar. Pet. Geol.* **2024**, *165*, 106858.
62. Schwartz, T.M.; Graham, S.A. Stratigraphic architecture of a tide–influenced shelf–edge delta, Upper Cretaceous Dorotea Formation, Magallanes–Austral Basin, Patagonia. *Sedimentology.* **2015**, *62*, 1039–1077.

63. Kumar, P.; Devi, K.L.; Chakraborty, P.P.; Rajkumar, H.S. Depositional architecture of sub–aqueous part of a tide–dominated delta and its palaeogeographic implications: Laisong Formation (Barail Group), Indo–Myanmar Ranges, western Manipur. *J. Earth Syst. Sci.* **2022**, *131*, 103.
64. Dashtgard, S.E.; Gingras, M.K.; MacEachern, J.A. Tidally modulated shorefaces. *J. Sediment. Res.* **2009**, *79*, 793–807.
65. Gong, Z.J.; Li, Q.W.; Luo, M.; Dai, C.C.; Peng, H.M. Sedimentary facies and chronological study for a Late Pleistocene sand layer with swash cross bedding within a sand hill at north of Poyang Lake, as inferred from sedimentary structure and optical dating of K–feldspar and quartz grains. *Quat. Int.* **2023**, *673*, 29–39.
66. Hovikoski, J.; Uchman, A.; Weibel, R.; Nohr–Hansen, H.; Sheldon, E.; Ineson, J.; Bjerager, M.; Therkelsen, J.; Olivarius, M.; Larsen, M.; et al. Upper Cretaceous bottom current deposits, north–east Greenland. *Sedimentology* **2020**, *67*, 3619–3654.
67. Huang, Y.T.; Tan, X.F.; Liu, E.T.; Wang, J.; Wang, J.P. Sedimentary processes of shallow–marine turbidite fans: An example from the Huangliu Formation in the Yinggehai Basin, South China Sea. *Mar. Pet. Geol.* **2021**, *132*, 105191.
68. Blanchard, S.; Matheson, E.J.; Fielding, C.R.; Best, J.L.; Bryk, A.B.; Howell, K.J.; Monson, C.C.; Mahoney, G.; Peakall, J. Early burial mud diapirism and its impact on stratigraphic architecture in the Carboniferous of the Shannon Basin, County Clare, Ireland. *Sedimentology* **2019**, *66*, 329–361.
69. Liu, Z.S.; Li, L.Q.; Wang, Y.D. Sporopollen assemblage of the Late Triassic in Xuanhan, Sichuan Province and its paleovegetation and paleoclimate significance. *Acta Micropalaeontol. Sin.* **2015**, *32*, 43–62, (In Chinese with English Abstract).
70. Zheng, R.C.; Li, G.H.; Chang, H.L.; Li, S.L.; Wang, X.J.; Wang, C.Y. Sedimentary sequence and paleogeographic characteristics of the Upper Triassic Xujiahe Formation in eastern Sichuan basin. *Geol. China* **2015**, *42*, 1024–1036. (In Chinese with English Abstract)
71. Pole, M.; Wang, Y.D.; Dong, C.; Xie, X.P.; Tian, N.; Li, L.Q.; Zhou, N.; Lu, N.; Xie, A.W.; Zhang, X.Q. Fires and storms–a Triassic–Jurassic transition section in the Sichuan Basin, China. *Palaeobiodivers. Palaeoenviron.* **2018**, *98*, 29–47. [CrossRef]
72. Li, L.Q.; Wang, Y.D. Late Triassic palynofloras in the Sichuan Basin, South China: Synthesis and perspective. *Palaeoworld* **2016**, *25*, 212–238. [CrossRef]
73. Li, L.Q.; Wang, Y.D.; Vajda, V.; Liu, Z.S. Late Triassic ecosystem variations inferred by palynological records from Hechuan, southern Sichuan Basin, China. *Geol. Mag.* **2018**, *155*, 1793–1810.
74. Lu, N.; Wang, Y.D.; Popa, M.E.; Xie, X.P.; Li, L.Q.; Xi, S.N.; Xin, C.L.; Deng, C.T. Sedimentological and paleoecological aspects of the Norian-Rhaetian transition (Late Triassic) in the Xuanhan area of the Sichuan Basin, Southwest China. *Palaeoworld* **2019**, *28*, 334–345. [CrossRef]
75. Chen, H.D.; Li, J.; Zhang, C.G.; Cheng, L.X.; Cheng, L.J. Discussion of sedimentary environment and its geological enlightenment of Shanxi Formation in Ordos Basin. *Acta. Petrol. Sin.* **2011**, *27*, 2213–2229.
76. Dashtgard, S.E.; Wang, A.H.; Pospelova, V.; Wang, P.L.; La Croix, A.; Ayranci, K. Salinity indicators in sediment through the fluvial–to–marine transition (Fraser River, Canada). *Sci. Rep.* **2022**, *12*, 14303.
77. Lei, B.J.; Que, H.P.; Hu, N.; Niu, Z.J.; Wang, H. Geochemistry and sedimentary environments of the Palaeozoic siliceous rocks in western Hubei. *Sediment. Geol. Tethyan Geol.* **2002**, *22*, 70–79, (In Chinese with English Abstract).
78. Shi, Z.S.; Zhou, T.Q.; Guo, C.M. Clastic sedimentary records of the Upper Triassic Sichuan Basin, China: Implications for the transition from marine to transitional environment. *Geol. J.* **2022**, *57*, 4393–4411. [CrossRef]
79. Jones, B.; Manning, D.A.C. Comparison of geochemical indices used for the interpretation of palaeoredox conditions in ancient mudstones. *Chem. Geol.* **1994**, *111*, 111–129. [CrossRef]
80. Nie, Y.; Fu, X.G.; Xu, W.L.; Wen, H.G.; Wang, Z.W.; Song, C.Y. Redox conditions and climate control on organic matter accumulation and depletion during the Toarcian in the Qiangtang Basin, eastern Tethys. *Int. J. Earth. Sci. (Geol. Rundsch.)* **2020**, *109*, 1977–1990.
81. Gu, J.L.; Zheng, R.C.; Luo, P.; Yang, Z.X. Sequence stratigraphic framework and source–reservoir–cap rock of Xujiahe Formation in West Sichuan depression. *J. CDUT-Sci. Technol. Ed.* **2004**, *31*, 282–290, (In Chinese with English Abstract).
82. Lin, L.B.; Chen, H.D.; Jiang, P.; Hu, X.-Q. Sedimentary Facies and Lithofacies Paleogeographic Evolution of the Xujiahe Formation in the Western Sichuan Foreland Basin. *J. Chengdu Univ. Technol. (Sci. Technol. Ed.)* **2006**, *33*, 376–383. (In Chinese with English Abstract)
83. Wang, L.J.; Zhang, G.C.; Li, C.Q. Reservoir Characteristic of Triassic Jia' er1–Jiayi Gas Pool of Baoyuan Structure, Chishui, Guizhou. *Guizhou Geol.* **2004**, *79*, 94–98, (In Chinese with English Abstract).
84. Zhang, Z.; Zeng, W.; Yang, X.Y. The Division and Distribution of Diagenetic Facies of Xujiuhe Formation in Upper Triassic, Southern Sichuan. *J. SWPU-Sci. Technol. Ed.* **2006**, *28*, 13–15+23+112, (In Chinese with English Abstract).
85. Jiang, Z.X.; Tian, J.J.; Chen, G.J.; Li, X.Z.; Zhang, M.L. Sedimentary characteristics of the Upper Triassic in western Sichuan foreland basin. *J. Palaeogeogr.* **2007**, *9*, 143–154, (In Chinese with English Abstract).
86. Gao, Z.Y.; Han, G.M.; Zhang, L.H. Parasequence of fluvial deposit:a case study of the Xujiahe Formation in Central Sichuan. *Oil Gas Geol.* **2007**, *28*, 59–68. (In Chinese with English Abstract)
87. Liu, J.H.; Zhang, S.Q.; Sun, Y.T.; Wei, C.G. Correlation and Evolution of the Upper Triassic Xujiahe Formation in the West Sichuan Foreland Basin. *J. Stratigr.* **2007**, *31*, 190–196. (In Chinese with English Abstract)

88. Hou, F.H.; Jiang, Y.Q.; Fang, S.X.; Guo, G.A.; Yang, J.L. Sedimentary model of sandstone in second and fourth members of Xiangxi Formation in the Upper Triassic of Sichuan Basin. *Acta Pet. Sin.* **2005**, *26*, 30–37. (In Chinese with English Abstract)
89. Zhao, X.F.; Lu, Z.G.; Zhang, W.L.; Peng, H.R.; Kang, R.D. Paralic tidal deposits in the Upper Triassic Xujiahe Formation in Anyue area, the Sichuan Basin. *Nat. Gas Ind.* **2008**, *28*, 14–18+134. (In Chinese with English Abstract)
90. Lai, W.; Ruan, Z.; Wang, L.D.; Shen, Z.H. Geochemical Characteristics and Geological Significance of Mudstones from the Xujiahe Formation in the Qilixia Section, Northeastern Sichuan Basin. *Acta Petrol. Mineral.* **2019**, *38*, 657–672. (In Chinese with English Abstract)
91. Wu, Y.P.; Liu, C.L.; Jiang, F.J.; Hu, T.; Zhang, C.X.; Lv, J.H.; Hu, M.L.; Huang, R.D.; Wu, G.Y.; Awan, R.S. Hydrocarbon generation and expulsion of the Fengcheng Formation in the Mahu sag, Junggar Basin, China: Implications for shale oil resource potential. *Interpret.-J. Sub.* **2023**, *11*, T145–T159.

Disclaimer/Publisher's Note: The statements, opinions and data contained in all publications are solely those of the individual author(s) and contributor(s) and not of MDPI and/or the editor(s). MDPI and/or the editor(s) disclaim responsibility for any injury to people or property resulting from any ideas, methods, instructions or products referred to in the content.